The completion of this thesis
was supported by the
Randy Seeling Award
given, in his memory, to another
outstanding graduate student
of the Geology Department,
University of Minnesota, Duluth.

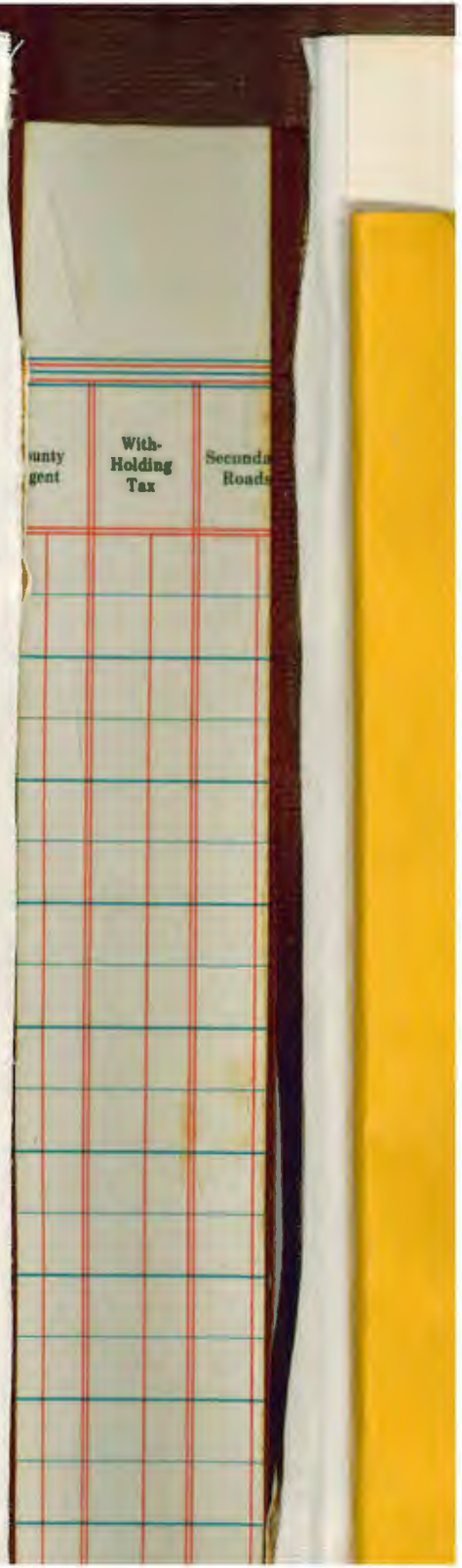

A COMPARISON OF TWO ARCHEAN ULTRAMAFIC PYROCLASTIC ROCK UNITS FROM THE SUPERIOR PROVINCE, NORTHWESTERN, ONTARIO

A THESIS
SUBMITTED TO THE FACULTY OF THE GRADUATE SCHOOL
OF THE UNIVERSITY OF MINNESOTA
BY

Stephen Jon Schaefer

IN PARTIAL FULFILLMENT OF THE REQUIREMENTS
FOR THE DEGREE OF
MASTER OF SCIENCE

December, 1989

Abstract

Two Archean komatiitic pyroclastic rock units occur on opposite sides of the Quetico Fault in northwestern Ontario. The eastern unit, the Dismal Ashrock is located 3 km north of Atikokan, Ontario on the northern side of the Quetico fault within the Wabigoon Subprovince of the Superior Province. It is part of a supracrustal sequence (the Steep Rock Group) that overlies an Archean unconformity. The Grassy Portage Bay Ultramafic pyroclastic rock unit (GUP) is located 100 km to the west on the south side of the Quetico fault, and is part of an overturned succession comprising mafic metavolcanic rocks, GUP and metasedimentary rocks. The Quetico Fault is a dextral fault with a history of transpressive tectonics.

The Dismal Ashrock is steeply inclined, little deformed and has undergone greenschist facies metamorphism, and it is divided into komatiitic lapilli tuff, komatiitic volcanic breccia, komatiitic volcaniclastic rocks and a mafic pillowed flow. The GUP outcrops form an arcuate fold interference pattern. The GUP is strongly deformed and has undergone amphibolite facies metamorphism. It is divided into komatiitic lapilli tuff and komatiitic volcanic breccia.

The Dismal Ashrock and the GUP contain cored and composite lapilli - unequivocal evidence for explosive volcanism. Locally some of the lapilli fragments are highly vesicular (up to 30% by volume) - greater than reported for any other komatiites. Other fragments show no vesicularity. The low vesicularity of some of the pyroclasts and association with pillowed lava flows in the case of the Dismal Ashrock indicate phreatomagmatic volcanic activity. Explosive water-magma interaction was probably initiated by modified eruption characteristics produced from exsolving volatiles.

The Dismal Ashrock and GUP are similar in chemical composition and plot on the border between peridotitic and basaltic komatiites on a Jensen AFM diagram. They are high in MgO, Cr and Ni; however, they are unusually enriched in Fe, Ti, Zr, Mn, P, Ba, Nb, Rb and Sr compared to other komatiites. Several lines of evidence indicate that this unusual composition could not have been caused by alteration or assimilation, and an enriched mantle source region is the likely cause.

Many of the characteristics that Dismal Ashrock and GUP share are rare or unique on a global scale, indicating that the Dismal Ashrock and GUP are correlative in some manner.

Acknowledgements

The author gratefully acknowledges his thesis advisor Dr. Penelope Morton of University of Minnesota, Duluth and Dr. H. K. Poulsen of the Canadian Geolgical Survey for their guidance on this project.

Dr. John Green, Dr. Tim Holst and Dr. Paul Siders are thanked for serving as members of the adivisory committee for this thesis.

The faculty and my peers in the Geology Department at the University of Minnesota, Duluth are appreciated for providing a stimulating environment.

The Geological Survey of Canada and The Geological Society of America are acknowledged for their generous financial support of this thesis. The Ontario Geological Survey is thanked for their field support. The Ministry of Natural Resources, Atikokan provided access to the old Steep Rock Mine.

Special thanks goes to my parents Dr. Donald and Anna Marie Schaefer for their support and encouragement.

Table of Contents

List of Figures, Plates, and Tables

List of Plates

List of Tables

I. INTRODUCTION

I.1 Purpose of Study

Komatiites have been the subject of intense research since their description twenty years ago (Viljoen and Viljoen, 1969). Only recently have descriptions of pyroclastic komatiites appeared in the literature (Gelinas, Lajoie, and Brooks, 1977; Saverikko, 1983; Echeverria and Aitken, 1986). Two such pyroclastic komatiitic rock units exist in northwestern Ontario. One unit, the Dismal Ashrock, occurs in the Steep Rock Group (Wilkes and Nisbet, 1987) north of Atikokan; the other occurs on the eastern portion of Rice Bay Dome, 20 km east of Fort Francis.

The purpose of this study is four-fold. First, to provide a detailed description and comparison of the chemical and physical aspects of these two units. Second, determine if they are correlative, as has been suggested by Howard Poulsen (pers. comm., 1988). The two units occur on opposite sides of the dextral Quetico fault and are about 100 km apart (Fig. 1). Third, describe the volcanic stratigraphy of the rock units, to determine the environmental and physio-chemical factors that were involved in creating explosive volcanism in these magmas. Finally, relate the above parameters to mantle conditions and tectonic processes in this region.

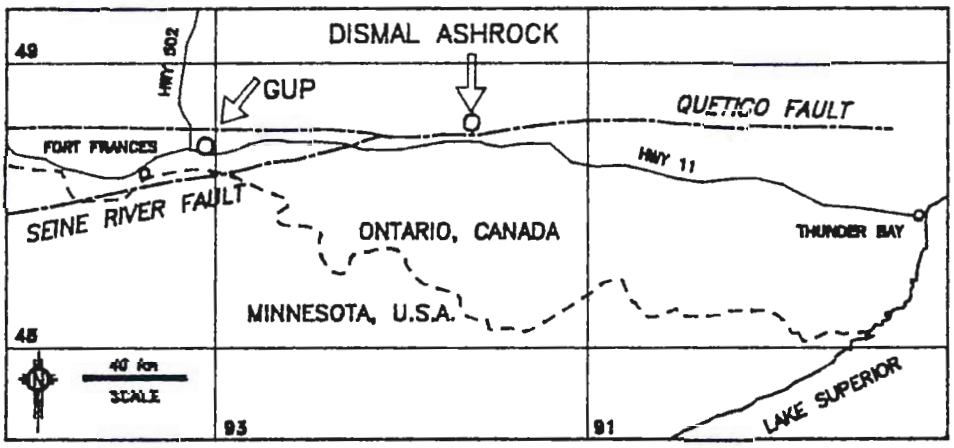

Figure 1. Location of the Dismal Ashrock and the Grassy Portage Bay Ultramafic Pyroclastic Rock Unit (GUP) relative to the Quetico Fault.

I.2 Location

The komatiitic pyroclastic rock units are located in the northwestern portion of Ontario, Canada (Fig. 1). The Dismal Ashrock crops out 4 kilometers north of Atikokan in what was formerly Steep Rock Lake (Fig. 2). Access is by Highway 11B north of Highway 11. Exposure of the unit occurs in two former iron mines (Fig. 2). The western mine, the Steep Rock pit, has exposures of the Dismal Ashrock along the steep western walls of the pit. No exposures are found in the eastern mine, the Cayland pit, due to high water levels, however some exposures are found to the southeast. Water is filling both of the pits and exposure will decrease through time.

The second unit occurs 100 km to the west, 20 km east of Fort Francis on Highway 11 (Figs. 1 & 3). Outcrops occur along both shores of the northern portion of Grassy Portage Bay. This Grassy Portage Bay ultramafic pyroclastic rock unit (GUP) is also visible on Highway 11, 1.5 km west of the Highway 502 intersection and along Highway 502, 3 km north of Highway 11. Outcrops are also scattered throughout the hummocky terrain to the east of Highway 502 and north of Highway 11. Access to these interior portions can be obtained on foot by cut line or logging roads in some cases.

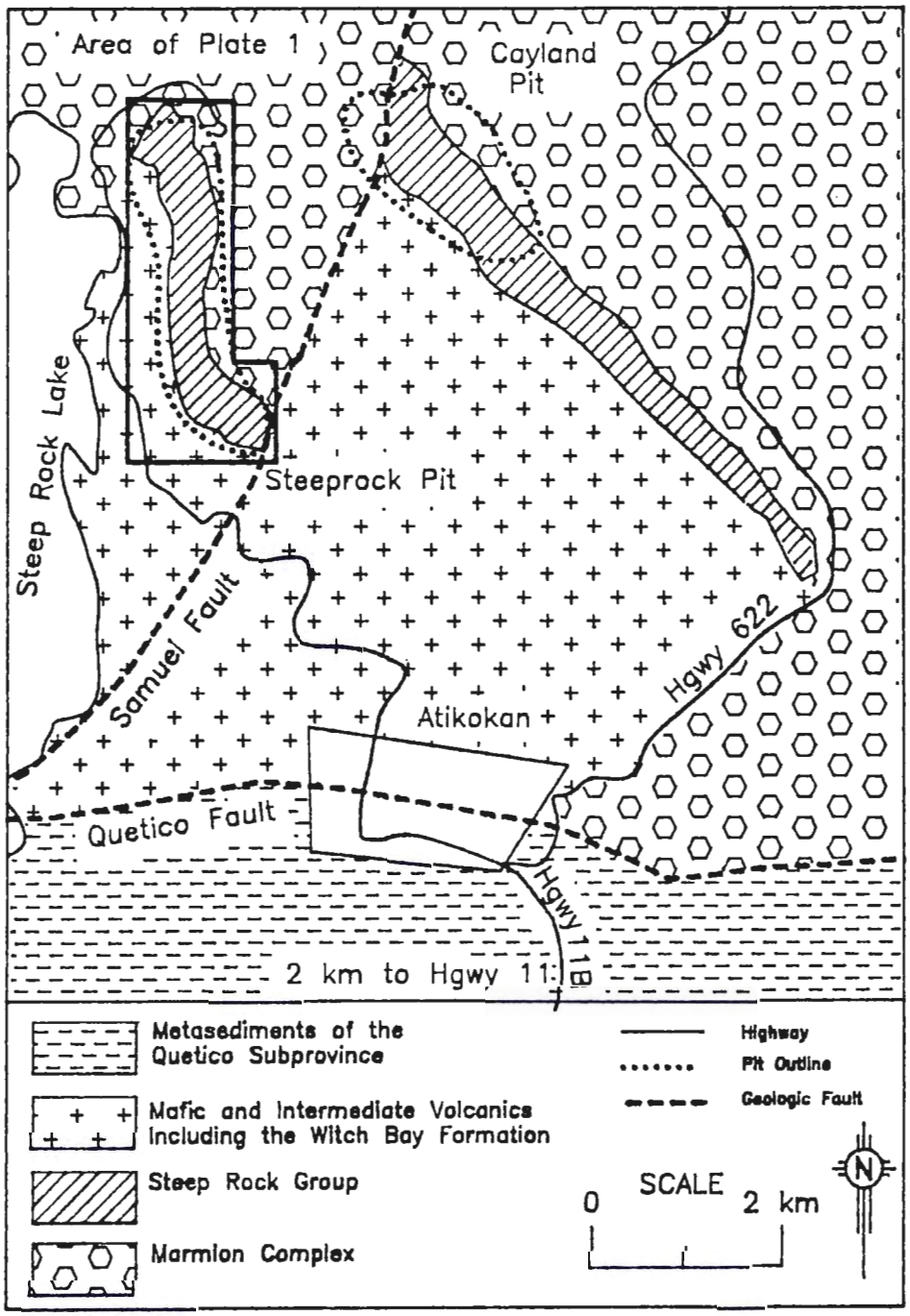

Figure 2. Location of the study area for the Dismal Ashrock, showing area of Plate 1. Geology after Shklanka (1972).

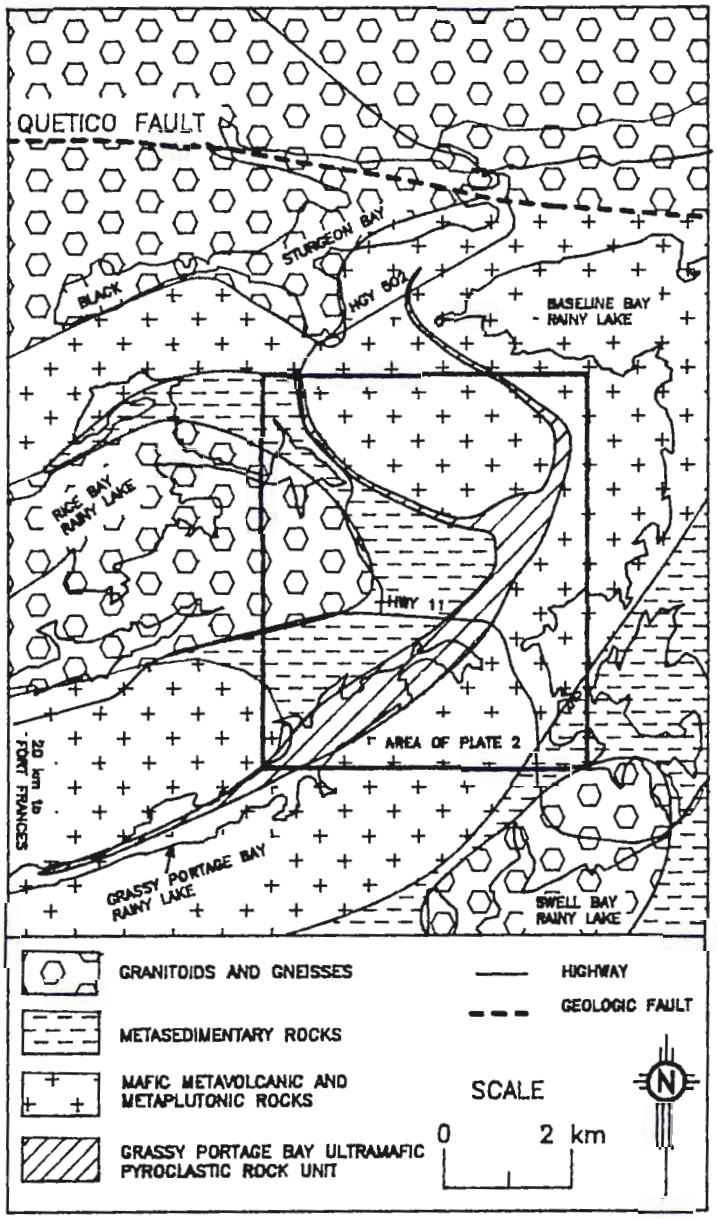

Figure 3. Location of the study area for the Grassy Portage Bay Ultramafic Pyroclastic Rock Unit (GUP), showing area of Plate 2. Geology after Poulsen (1984).

I.3 Methods

Detailed mapping of units and their contact relationships was done at scales from 1:50 to 1:10,000, and a stratigraphic column was made through a representative portion of the unit at Steep Rock. From this, geological maps showing the distribution of the Dismal Ashrock (1:5,000) and the GUP (1:10,000) were prepared (Plates 1 and 2). Thirty-eight thin sections were prepared from 36 representative samples and 55 samples, including four duplicates, were powdered in a alumina ceramic shatterbox and sent to X-Ray Assay Laboratories Limited of Toronto for major and selected trace element analysis. These analyses are used to compare the chemical composition of the Dismal Ashrock to the GUP and determine igneous and volcanic processes, as well as alteration processes, that occurred in the formation of these units. Volcanological interpretations are based on observed physical features, on all scales, by analogy with more recent and modern deposits.

I.4 Regional Geology

The two komatiitic pyroclastic rock units are exposed within the Superior Province of the Canadian Shield (Fig. 4). The Superior Province is divided into subprovinces based on lithology and structure (Card and Cieslieski, 1986). The Steep Rock Group occurs on the southern margin of the Wabigoon

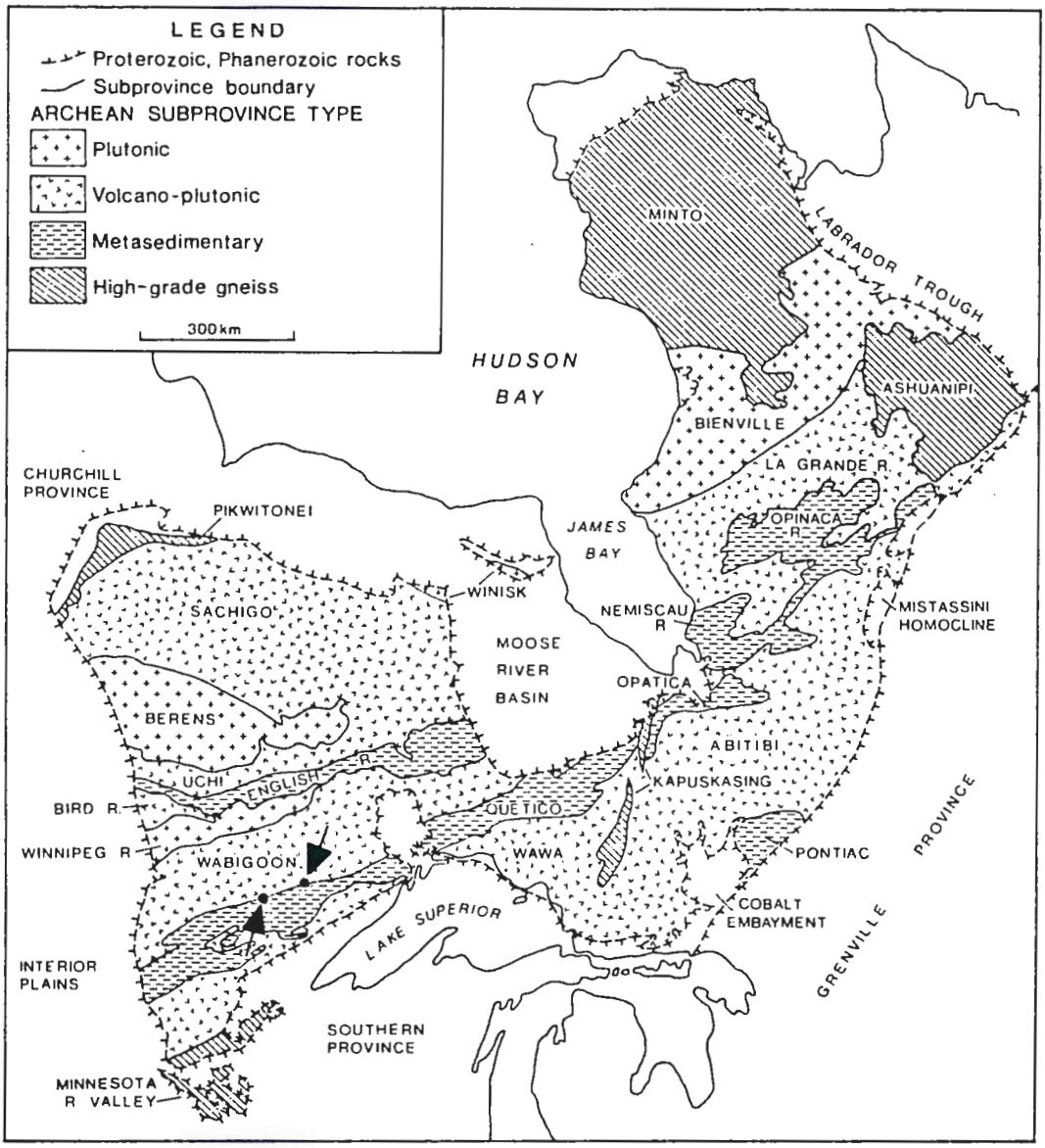

Figure 4. Location of the Dismal Ashrock and the GUP (arrows) relative to the Subprovinces of the Superior Province of the Canadian Shield (from Card and Ciesiskli, 1986).

Subprovince, which is a granite-greenstone terrain. This southern margin is defined by the Quetico Fault in this locale. On the southern side of the Quetico fault lies the Quetico Subprovince consisting of metasedimentary rocks. The GUP occurs in a transition region between the Wabigoon Subprovince and the Quetico Subprovince. This transition region is the area between the Quetico fault and the Seine River Fault (Poulsen, 1986) (Fig. 1). Poulsen (1986) has shown that this transition region has the characteristics of a transpression zone and that late stage dextral displacements on the Quetico fault might simply reflect this larger zone of wrenching.

Steep Rock

The ultramafic pyroclastic rock unit at Steep Rock is called the Dismal Ashrock and is part of a formally defined supracrustal sequence named the Steep Rock Group (Wilkes and Nisbet, 1987). There have been no direct age dates determined for the Steep Rock Group but it unconformably overlies a tonalite body to the northeast called the Marmion complex (Wilkes, 1986) which has been dated at 2991 Ma (Davis and Jackson, 1985). The Steep Rock Group consists of four formations, formally defined by Wilkes and Nisbet (1987), that form a homoclinal succession that is up to 1500 m thick and 12 km in strike length (Fig. 5). The following is a brief description of each unit, based on Wilkes and Nisbet's (1987)

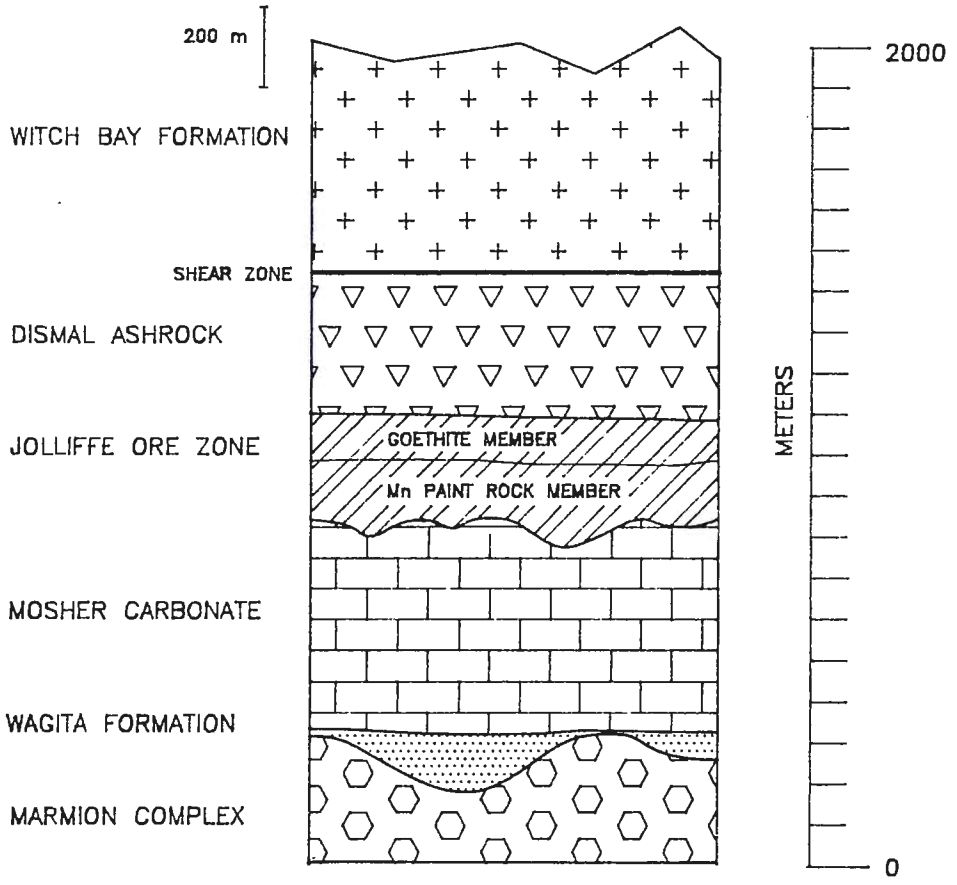

Figure 5. **An idealized section for the Steep Rock Group (from Wilkes, 1986).**

formal description, starting from the basal formation.

1) Wagita Formation: a clastic unit (0-150 m thick) that ranges from metaconglomerate to pelite. It unconformably overlies the Marmion complex.

2) Mosher Carbonate: a carbonate unit (0-500 m thick) that consists of calcite, ankerite and dolomite and contains abundant stromatolites. It has a gradational contact with the underlying Wagita formation and its upper contact resembles karst topography

3) Jollife Ore Zone: an iron ore unit (100-400 m thick) that is composed of a lower unconsolidated manganese-rich rock (Manganese Paint Rock Member) and an upper brecciated goethite-rich layer (Goethite Member).

4) Dismal Ashrock: a mafic to ultramafic pyroclastic rock unit (100-400 m thick).

The upper portions of the Dismal Ashrock are highly strained as are the overlying mafic and intermediate flows and tuffs of the Witch Bay Formation (Wilkes and Nisbet, 1987). These factors, suggesting a fault contact, caused Wilkes and Nisbet (1987) to place the Witch Bay Formation only provisionally in the Steep Rock Group.

Grassy Portage Bay Area

The GUP occurs on the outer eastern edge of the Rice Bay Dome in an arcuate fold interference pattern (Ramsay Type 3).

It is 800 m in maximum thickness and 10 km in strike length (Fig. 4). The Rice Bay Dome occurs in a fault block defined by the Quetico fault to the north and the Seine River fault to the south. This region is thought to be a transition zone between the Wabigoon subprovince and the Quetico subprovince (Poulsen, 1980).

The GUP is part of a lithostratigraphic unit called the Keewatin Volcanics which structurally overlies the Coutchiching metasediments (Lawson, 1913). In the Grassy Portage area the GUP is in contact with and on top of the Coutchiching metasedimentary rocks to the west and lies underneath mafic metavolcanic and intrusive rocks of the Keewatin to the east. There are no age dates for these units, however the Keewatin volcanics are older than the Coutchiching metasediments based on topping directions determined by graded and cross beds (Grout, 1933). Age dates for Keewatin volcanic rocks in other parts of the western Wabigoon Subprovince range from 2755-2695 Ma. (Blackburn, Bond, Breaks, Davis, Edwards, Poulsen, Trowell and Wood, 1985).

I.5 Previous Work

Steep Rock

The first description of the rocks at Steep Rock was written in 1891 by Smyth. Smyth described nine formations in a steeply dipping homoclinal succession, in what he called the

Steep Rock Series. The unit now called the Dismal Ashrock, he originally termed the interbedded crystalline traps. Smyth (1891) described the unit as greenish-grey interbedded eruptives. Smith (1893) and McInnes (1899) did reconnaissance work in the area but did not add to the description of the Dismal Ashrock.

In 1913 Lawson described the succession to include only the units from the Dismal Ashrock down to the unconformity over the tonalite. He felt the units above the Dismal Ashrock were Keewatin in age and should not be included in the Steep Rock Series and therefore used only four formations.

Bartley (1940) termed the ultramafic pyroclastic rock unit "ashrock" and provided a description:

> "... a pyritiferous, tuffaceous agglomerate of basic composition containing an abundance of iron sulphide nodules and andesitic bombs and a heterogeneous mixture of limestone, clastics and magnetic material." p. 39.

Jolliffe (1955) introduced the term Steep Rock Group and continued the use of the term ashrock for the Dismal Ashrock. His description is as follows:

> "... a typical specimen shows loosely-packed, dark green to black, lenticular, aphanitic serpentinized fragments averaging less than one

inch across in a greenish schistose matrix that may show white carbonate patches." p.383-385.

He also reported larger volcanic fragments up to a foot across and apparently altered granitic fragments up to three inches across. Furthermore, he reported serpentinized pillowed lava flows within the ashrock.

Jolliffe (1955) noticed that the ashrock had three distinct alteration types. First, there is a red and brown alteration of the ashrock, due to the development of hematite and limonite. In the second type the ashrock is "bleached" a very light green color. In the third type the ashrock is replaced by pyrite. Jolliffe originally believed that the pyrite zones were late stage hydrothermal features related to nearby granite intrusions (Marmion Complex). Jolliffe (1966) also mentioned the existence of one or more pillowed basic lava flows within the Dismal Ashrock.

Wright (1959, 1965) described two types of lenticular pyrite zones: 1. Consolidated pyrite that consisted of massive pyrite with up to 40% goethite and hematite and small lenses of carbonaceous material. 2. Unconsolidated pyrite consisting of angular to round fragments of pyrite with cryptocrystalline textures. He indicated that the pyrite zones in the ashrock might be sedimentary due to the Dismal Ashrock's association with cherty and carbonaceous sediments. However, Wilkes (1986)

uses this same evidence, along with its non-conformable nature to support a hydrothermal origin.

Jolliffe (1971) reported on the chemistry and petrography of the ashrock. He attempted to determine the original magma composition by subtracting H_2O, CO_2, SiO_2 and CaO, thought to be gained through alteration processes from whole rock analysis and his results are presented in Table 1. He also determined that the carbonate matrix in an "unaltered" sample of the Dismal Ashrock was calcite (<1% MgO).

Schklanka (1974) described the ashrock as an ultramafic pyroclastic rock consisting of tuff, lapilli tuff, and agglomerate. He reported that lapilli tuff was most common and was composed of fine-grained ferrostilpnomelane, chlorite and disseminated magnetite. He also reported that vesicles were numerous and filled with calcite or more rarely stilpnomelane, quartz and chlorite.

McIntosh (1974) reported on the ashrock in the Cayland Mine. He said that the ashrock in this region graded to the southwest into a "... fine grained black carbonate-rich rock lacking pyroclastic textures." p.89.

Wilkes and Nisbet (1987) formally defined the Steep Rock Group and gave the ashrock its now formal name of the Dismal Ashrock. Wilkes (1986) described the Dismal Ashrock as a mafic-ultramafic pyroclastic rock unit, with 15-20% MgO, that forms 90% of the formation. She reported two main fragment

Table 1

	wt%
SiO2	42.4
TiO2	2.2
Al2O3	8.1
Fe2O3	5.6
FeO	15.7
MnO	0.4
MgO	20.8
CaO	1.0
Na2O	0.2
K2O	0.8
P2O5	0.1
CO2	0.3
H2O+	2.0
Total	99.6
	ppm
Sc	50
V	223
Cr	1874
Co	94
Ni	1063
Cu	152
Zn	96
Sr	52
Y	14
Zr	137
Ba	32

Table 1. The original composition of the Dismal Ashrock as calculated by Jolliffe (1971).

types: first, round to subround clasts 1 cm to 6 cm in diameter, and second, volcanic blocks up to 7 m in length and 1 m in width. The clasts contain green acicular actinolite and relict augite and olivine crystals that show swallow-tail quench textures and abundant disseminated opaque minerals, magnetite and chromite. The groundmass consists of a mineral assemblage of serpentine with minor chlorite, calcite, quartz and actinolite. The volcanic blocks contain an assemblage of 40% amphibole crystals in a groundmass of chlorite, serpentine, opaque minerals and calcite. The matrix between the clasts and blocks is mostly calcite with minor actinolite, serpentine, chlorite, and pyrite.

Wilkes (1986) also described high-Mg mafic dikes and two sets of mafic dikes that intrude the Dismal Ashrock and lower units within the Steep Rock Group (Table 2). She described the high-Mg dikes as medium to coarse-grained olive green to grey rocks that consist of a mineral assemblage of actinolite crystals in a groundmass of chlorite, epidote and sphene. Wilkes also compared these dikes to volcanic blocks in the Dismal Ashrock. She found that the blocks and dikes had similar whole rock and amphibole compositions and speculated that the dikes represent possible feeders for the Dismal Ashrock. She described the mafic dikes as dark to pale green in color, coarse-to medium-grained. Their mineralogy varies from an assemblage of olivine and opaque minerals surrounded by

Table 2

	High-Mg Mafic Dikes	Mafic dikes
SiO2	47.97	50.22
TiO2	0.50	0.87
Al2O3	7.91	12.21
Fe2O3	10.30	11.88
MnO	0.15	0.19
MgO	22.24	10.14
CaO	7.47	9.35
Na2O	0.96	2.74
K2O	1.05	1.35
P2O5	0.55	0.60
total	99.10	99.58

Table 2 **Average of high-Mg mafic dikes and mafic dikes in the Steep Rock Group. (From Wilkes, 1986).**

actinolite, chlorite and serpentine to an ophitic texture originally composed of plagioclase (replaced by epidote) partially surrounded by psuedomorphs of actinolite after clinopyroxene.

Grassy Portage Bay Area

The rocks in the Grassy Portage area were first studied by Lawson (1913) who delineated the two major lithostratigraphic units: Coutchiching metasediments and Keewatin volcanics. He assumed that the Coutchiching metasediments were older because they are structurally underneath the Keewatin metavolcanic rocks. Grout(1933) determined on the basis of cross-bedding and graded bedding that the sequence was overturned and that the Keewatin metavolcanic rocks were older than the Coutchiching metasediments. The first description of the GUP is in Harris's 1974 report in which he reported that the unit was a magnetite-bearing lapilli-tuff and tuff. He estimated that the rock contained 10-15% disseminated magnetite and consisted of volcanic fragments from 1 mm - 30 mm in diameter.

Harris (1974) reported that the rock consisted of very fine plagioclase, quartz, amphibole, chlorite and magnetite. Chemical analysis of two samples showed silica contents of 40.6 and 31.9 wt %. He also reported a brown tuff which contained actinolite, chlorite, epidote, opaque minerals and quartz and

determined that the brown color is due to limonite stain.

Poulsen, Borradaile, and Kehlenbeck (1980) conclusively documented that the sequence in the Grassy Portage area was overturned, by using fold facing directions. In addition Poulsen (Pers. comm., 1988) noticed the gross similarity of the GUP and the Dismal Ashrock and suspected a possible correlation between the two units. He initiated a geochemical comparison that showed the GUP was indeed ultramafic and was broadly similar to the Dismal Ashrock. This present study began from this early work and has added new data and ideas to this intriguing proposition.

II. LITHOLOGY, STRATIGRAPHY AND VOLCANOLOGY

II.1 Introduction

The distribution of rock units found in the two field areas, Steep Rock and Grassy Portage area, are shown on Plates 1 and 2 respectively. Modal mineral abundances in thin section are listed in Appendix 1. The Dismal Ashrock has undergone greenschist facies metamorphism and the GUP has undergone amphibolite facies metamorphism, however for ease of discussion, the prefix meta will not be used throughout the remainder of the text. The stratigraphy, lithology and volcanology for the Dismal Ashrock and the GUP are discussed separately in the following sections.

II.2 Stratigraphy of the Dismal Ashrock

The Dismal Ashrock that crops out in the old Steep Rock mine is 3.6 km in strike length and 50 - 360 m thick, dips steeply (50 -80 degrees) to the west and strikes north -south (Plate 1). On the basis of field mapping the Dismal Ashrock is divided into the following units: komatiitic lapilli-tuff, komatiitic volcaniclastic rock, mafic lava flow and komatiitic volcanic breccia. The term volcanic breccia is used "sensu lato" and refers to a lapilli-tuff unit with block size fragments composing 5-20% of the unit.

A generalized section for the entire unit is shown in

Figure 6 and a detailed stratigraphic column for a portion of the Dismal Ashrock, measured in along A-A' in Plate 1 and Figure 6, is presented in Figure 7. The lower portion of the Dismal Ashrock consists of komatiitic lapilli tuff that is in contact for the entire 3.6 km length with the Jollife Ore Zone (Fig. 6). The komatiitic lapilli tuff is overlain in the southern part of the area by a thin (6 - 7 m) package of komatiitic volcaniclastic rocks and a thin (4 - 6 m) pillowed mafic flow (Figs. 6 and 7). The pillowed mafic flow is overlain by more komatiitic lapilli tuff. The komatiitic volcanic breccia is a small (25 x 100 m) elliptical shaped unit near the upper contact of the Dismal Ashrock (Fig. 6). The upper portion of the Dismal Ashrock consists of komatiitic lapilli tuff and volcanic breccia which are strongly foliated and in fault contact with the Witch Bay intermediate volcanics (Fig. 6). The fault contact is marked by a broad 5-20 m shear zone. Within this shear zone are small areas (<3 m thick) of carbonatized rock (samples SRE 211 and SRE 214; Appendix II) and bifurcating and anastomosing mafic dikes of varying thicknesses (0.25-3 m) (samples SRE 62 and SRE 217; Appendix II). Sample SRE 62 is from a lamprophyre dike that has visible biotite crystals in a dark-grey, fine-grained matrix. Sample SRE 217 is from a dark grey-green dike that is 50 cm wide.

Olive to dark green, non-magnetic, mafic dikes are also found below the shear zone within the Dismal Ashrock and Mosher

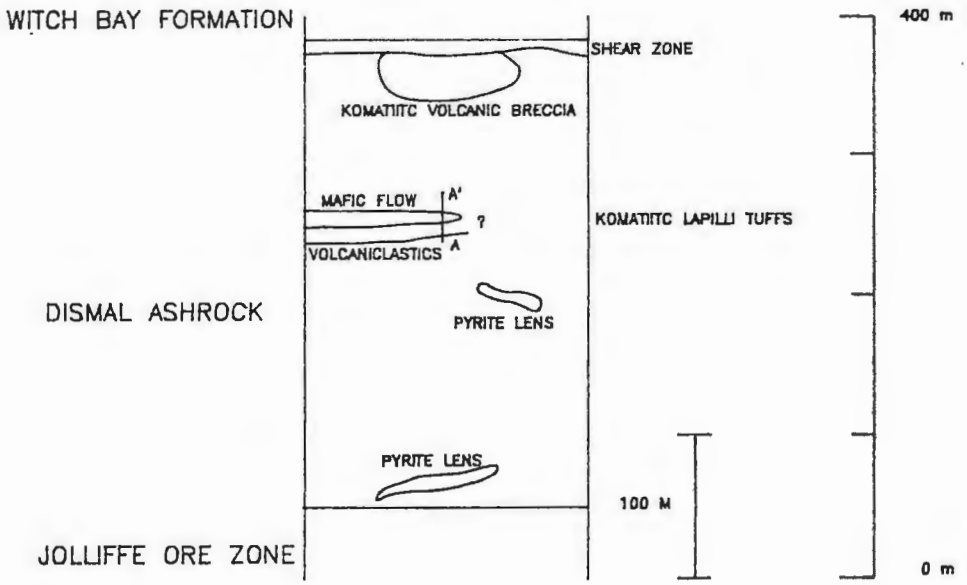

Figure 6. **An idealized section for the Dismal Ashrock. A-A' denotes the vertical location of the detailed stratigraphic column presented in Figure 7.**

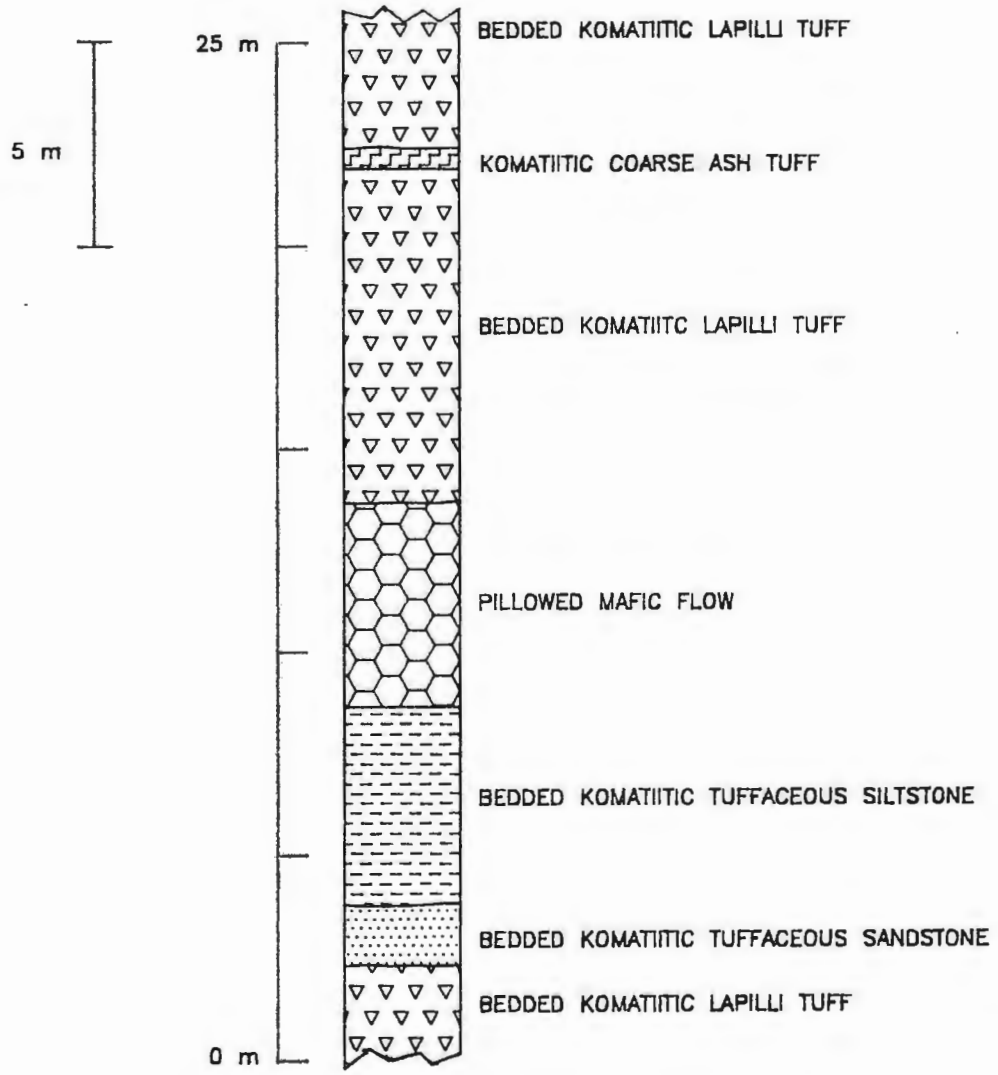

Figure 7. A detailed stratigraphic column for a portion of the Dismal Ashrock. Its location is marked by A-A'on Plate 1 and Figure 6.

Carbonate units (samples SRE 8 and SRE 84 respectively; Appendix I and II). Sample SRE 8 is from a 40cm wide dike within the Dismal Ashrock that consists of a fine-grained (<0.1mm) assemblage of foliated chlorite and actinolite with minor amounts of oxide, carbonate, sphene and quartz. The quartz and carbonate are concentrated in thin (1mm) vienlets. Sample SRE 84 is from a 3 m wide dike within the Mosher Carbonate. This dike is considerably altered and consists of a fine-grained (<0.2mm) assemblage of chlorite, quartz and calcite with minor oxides and actinolite. Some of the calcite forms euhedral crystals up to 3 mm across.

II.3 Description of the Lithologic Units of the Dismal Ashrock

Komatiitic Lapilli Tuff

The komatiitic lapilli tuff composes over 80% of the Dismal Ashrock and in outcrop consists of dark green-grey to grey-black rounded to angular, magnetic fragments in a white to light green matrix (Fig. 8). The fragments compose 60 - 90% of the rock and range in size from 1 mm to 6 cm; most are under 3 cm in diameter. Beds of varying thickness (2 - 15 cm) are common and are distinguished by a layer of coarse rounded fragments at the tops of the beds. Some minor beds are virtually devoid of lapilli size fragments and others are composed of over 75% lapilli tuff; they are classified as

Figure 8. A photograph of bedding in the lapilli tuff of the Dismal Ashrock; note the light-colored carbonate matrix between the pyroclasts.

coarse ash tuff and lapillistone, respectively.

Amygdules (from <0.05 to 2 mm in diameter) compose from 0 to 30% by volume, of the fragments (Fig. 9). The vast majority of fragments have amygdules or a fluidal or round shape that indicate that they are juvenile fragments. However, other fragments are angular of blocky in nature. Minerals in the fragments range from small (<0.3 mm) skeletal olivines (Fig. 10) pseudomorphed by serpentine, surrounded by optically unresolvable reddish brown to black material that might represent devitrified glass, to a fine-grained (<.1 mm) assemblage of actinolite (5-44%), opaque minerals (10-20%), serpentine (5-30%) and chlorite (5-34%) with no primary crystal forms visible (Fig. 11). The actinolite is colorless to pale green and forms small (<1 mm) long needles. The opaque minerals range from small (<0.1 mm) equant crystals (magnetite?) to small elongate laths (ilmenite?) <0.1mm in length and the remainder of the groundmass consists of a very fine-grained (<.1 mm) mat of pale green-yellow serpentine, chlorite and actinolite. The matrix surrounding the fragments and the material filling the amygdules consists of an assemblage of carbonate (80-90%) with minor chlorite, actinolite and talc. The carbonate species was determined by x-ray diffraction of powdered whole rock samples and it is typically calcite, however in two samples the carbonate has a dolomite crystal structure.

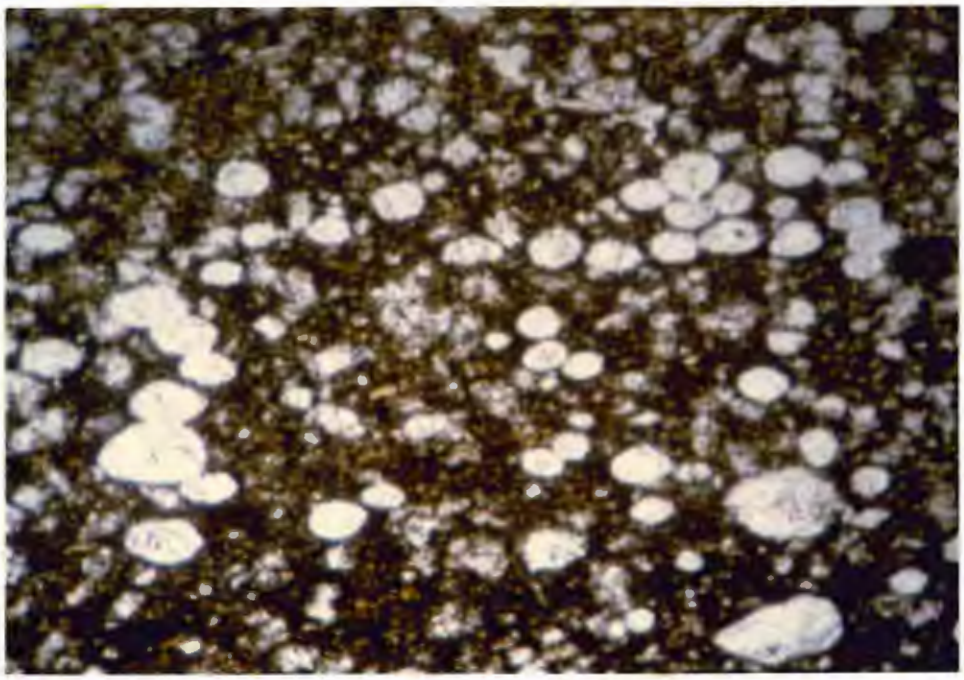

Figure 9. A photomicrograph of calcite amygdules in a juvenile pyroclast from the Dismal Ashrock. Plane polarized light, field of view 0.8 x 0.5 mm.

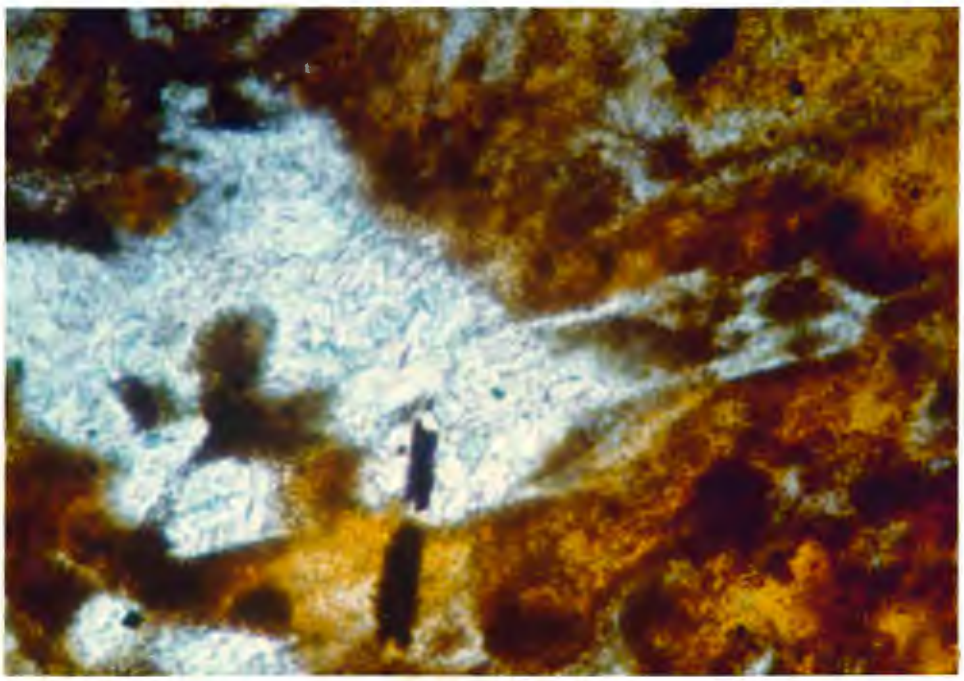

Figure 10. A photomicrograph of skeletal olivines pseudomorphed by serpentine from the Dismal Ashrock unit. Plane polarized light, field of view 0.3 x 0.2 mm.

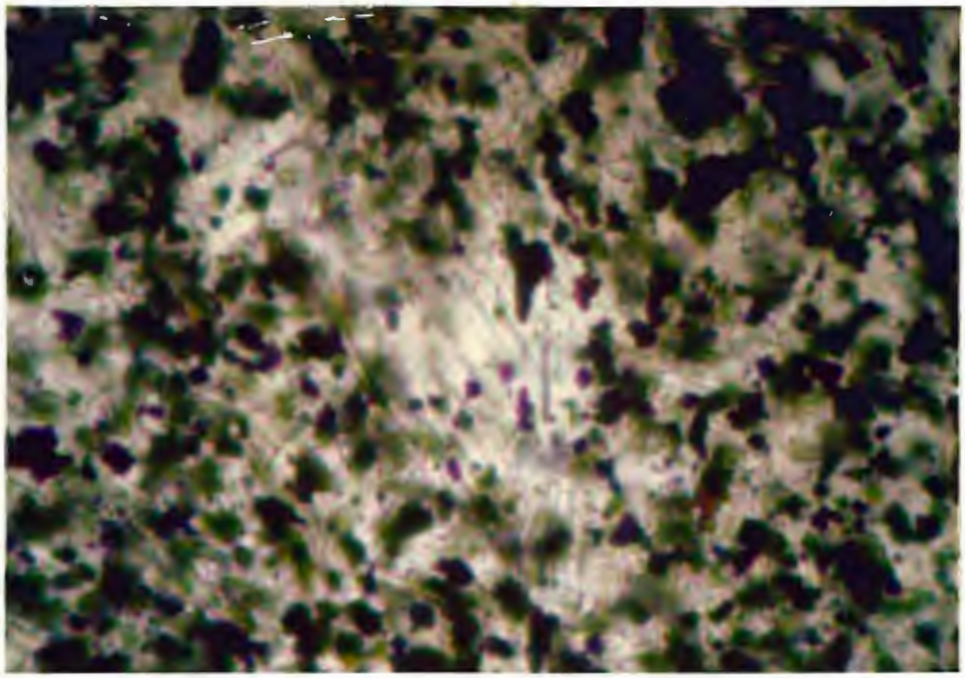

Figure 11. A photomicrograph of actinolite (colorless) and oxides (black to grey) in a pyroclast from the Dismal Ashrock. Plane polarized light, field of view 0.3 x 0.2 mm.

Two unusual juvenile fragment types are recognized. First, there are cored lapilli - fragments consisting of a core of juvenile or accidental material surrounded by a rind of quenched magma (Fig. 12). Second, there are composite lapilli - fragments consisting of a rind of quenched magma surrounding multiple lapilli-size fragments (Fig. 13). The cored lapilli can compose up to 5% of a sample whereas the composite lapilli are rare. One cored lapillus 5 mm in diameter has a quenched rim of magma that contains skeletal crystals 0.2 mm long in the interior portion of the rim and in the distal portion of the rim, microspinifex crystals 0.05 to 0.1 mm in length aligned sub-perpendicular to the rim surface (Figs. 14, 15).

Cognate fragments are found in the Dismal Ashrock. They are olive green in color, sub-round to angular, weakly to non-magnetic and vary in size from 2 cm to 4 cm. In thin section they are composed of a fine-grained assemblage of serpentine (40%), actinolite (35%), opaques (18%), chlorite (3%) and sphene (3%). Acicular crystals (olivine ?), 0.5 to 1mm long that are psuedomorphed by serpentine compose 10 - 20% of the rock (Fig. 16). Very rare accidental fragments are found within the komatiitic lapilli tuff and consist of carbonate and tonalite fragments. The carbonate fragments are white to pale green, angular to rounded and range in size from 1-3 cm in diameter (Fig. 17). They consist of small (0.1 -1 mm) anhedral

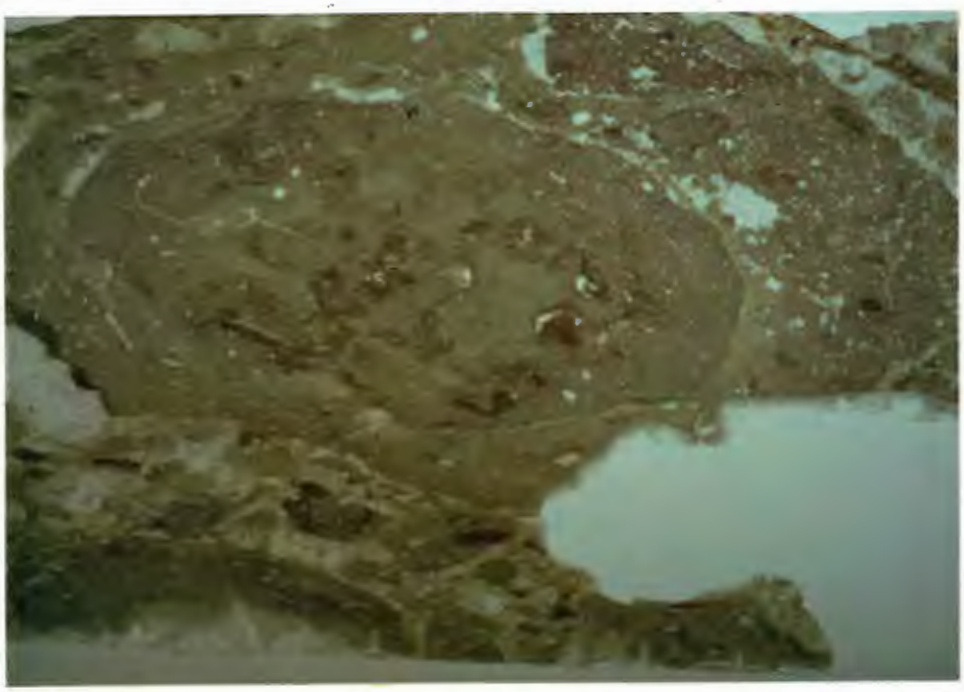

Figure 12. A photograph of a petrographic slide of the Dismal Ashrock lapilli tuff that contains a cored lapillus. Field of view 3.5 x 2 cm.

Figure 13. Photograph of a composite lapillus, 3 cm in diameter (arrow) in the Dismal Ashrock.

Figure 14. A photograph of a petrographic slide of the Dismal Ashrock lapilli tuff that shows a small broken cored lapillus partially included within another juvenile fragment. The small cored lapillus contains a core of vesiculated material and a dark rim with skeletal and microspinifex crystals (see below). Field of view 3 x 2 cm.

Figure 15. A photomicrograph of the outer rim of the cored lapillus in figure 14. Note the microspinifex crytals radiating from the outer edge of the rim (bottom of the picture). Plane polarized light, field of view 0.3 x 0.2 mm.

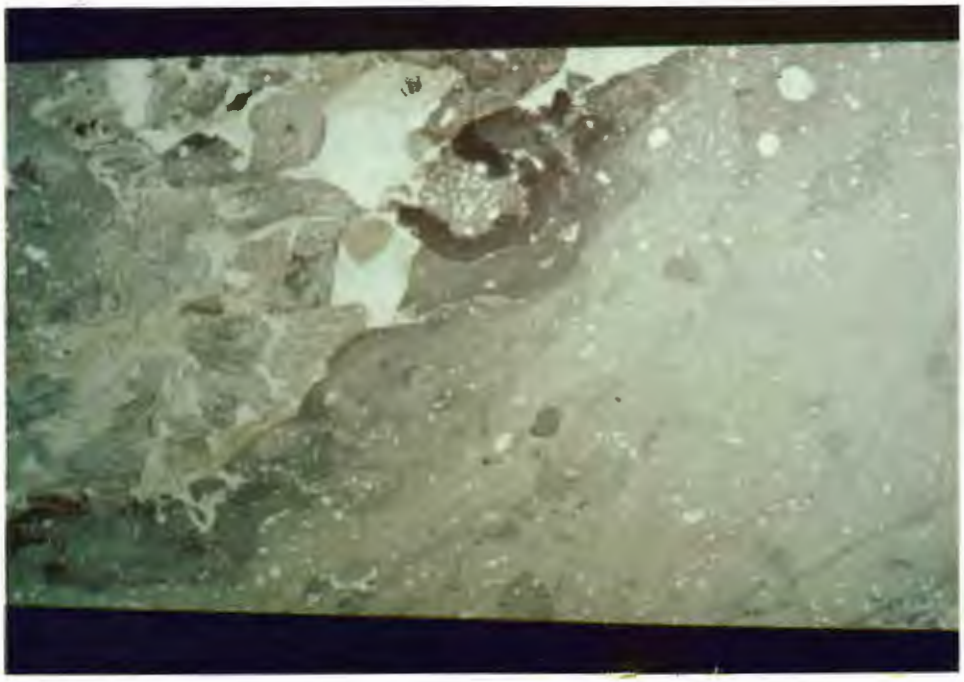

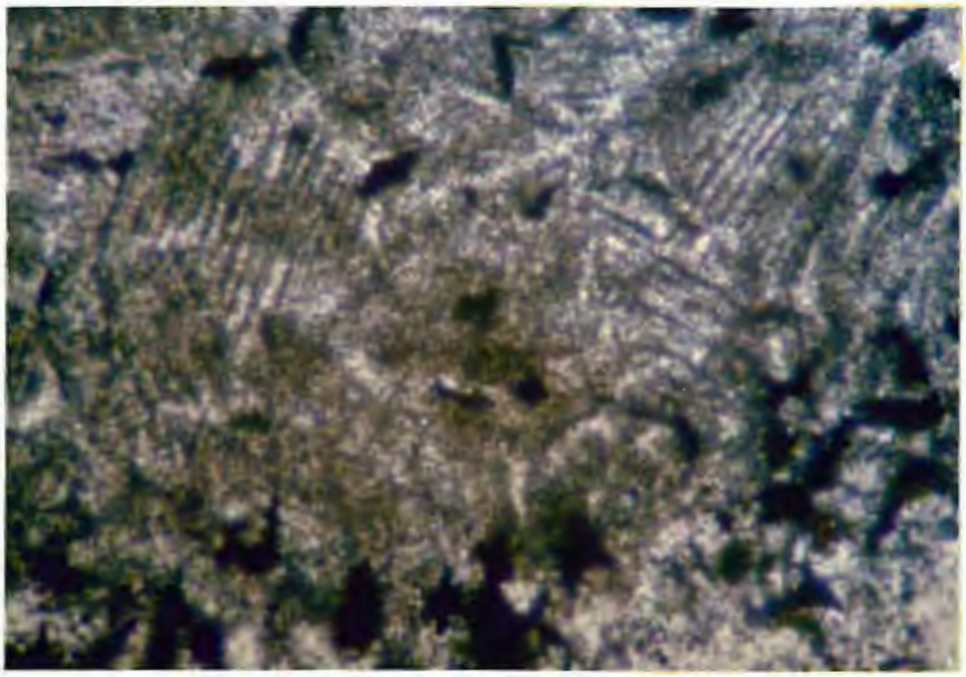

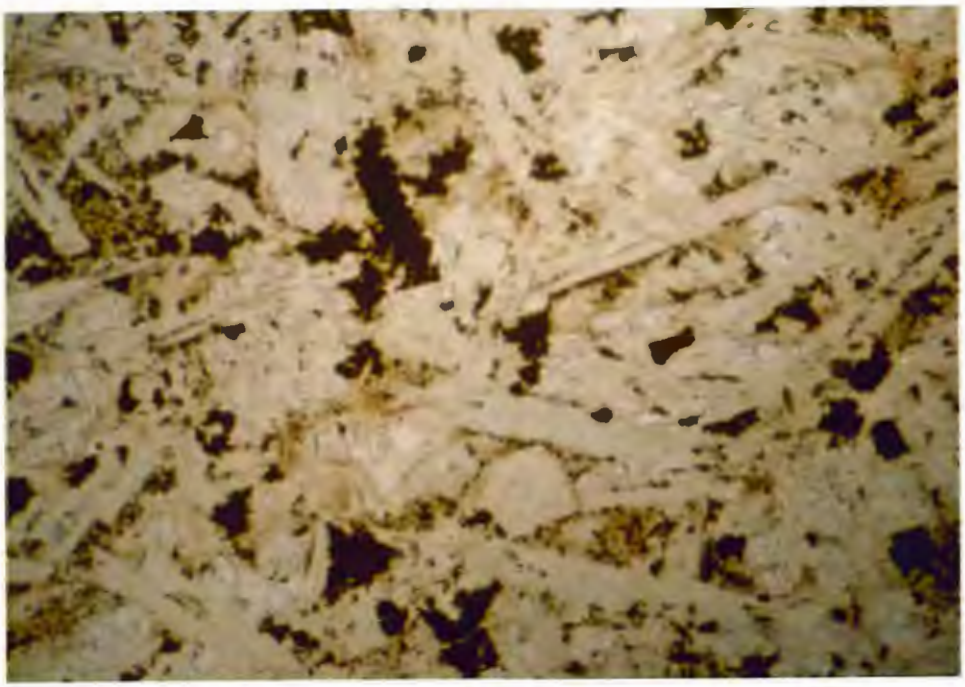

Figure 16. A photomicrograph of a cognate fragment in the Dismal Ashrock. Note the acicular crystals pseudomorphed by serpentine. Plane polarized light, field of view 0.8 x 0.5 mm.

Figure 17. A rock slab from the Dismal Ashrock that contains an accidental carbonate fragment (fragment is 1.5 cm in diameter).

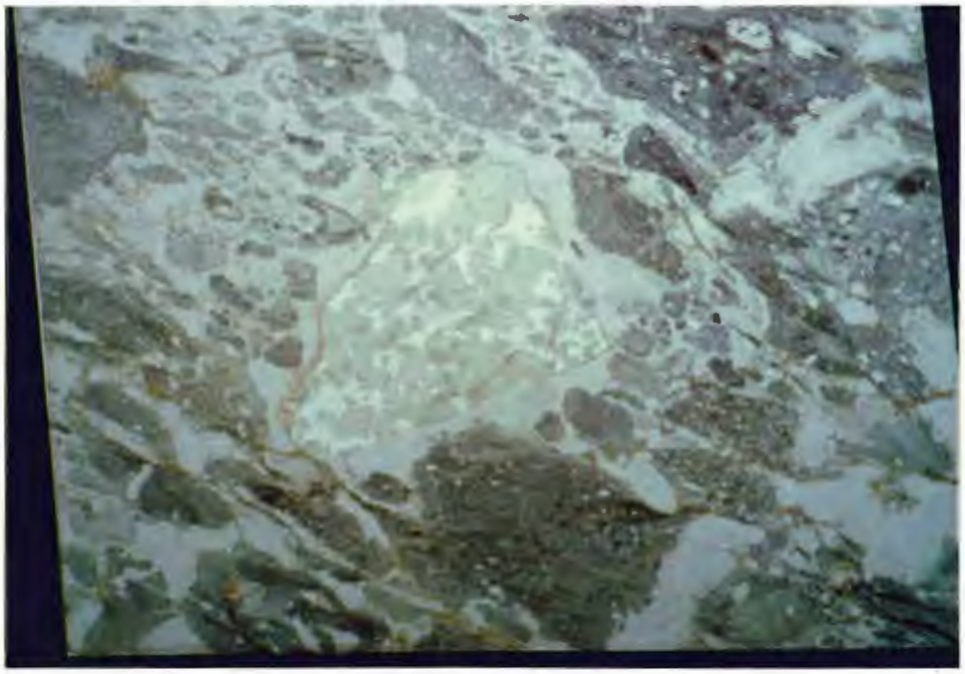

Figure 18. A photograph of a petrographic slide of the Dismal Ashrock that contains an accidental tonalite fragment. Field of view 3 x 2 cm.

calcite crystals with minor amounts of a pleochroic blue-green clinoamphibole and serpentine. The tonalite fragments are grey, sub-angular and range in size from 1-3 cm (Fig. 18). They are composed of over 60% plagioclase crystals that range in size from 1 to 5 mm and have been almost totally replaced by sericite and chlorite. Interstitial small (<0.6 mm) quartz grains with undulose extinction surround the plagioclase crystals.

Komatiitic Volcaniclastic Rock

The komatiitic volcaniclastic rocks are primarily found in the southern portion of the field area in a 6 - 7 m thick fining-upward sequence that grades from bedded tuffaceous sandstone to siltstone. However, there is also minor (<10 cm thick and <10 m in strike length) intercalation of tuffaceous siltstone in the central portion of the Steep Rock pit. The lower portion of the fining-upward sequence consists of green- and white-bedded tuffaceous sandstone that is composed of green subangular fragments (<2 mm in size) set in a white calcite matrix. The calcite matrix composes over 30% of the rock (Fig. 19). In thin section the fragments consist of a fine-grained (<0.1 mm) assemblage of serpentine, opaque minerals and chlorite.

The tuffaceous sandstone grades up into grey and white, laminated to thinly bedded (1 mm - 3 cm) tuffaceous siltstone

Figure 19. A rock slab of tuffaceous sandstone from the Dismal Ashrock; note the light colored carbonate matrix. Coin is 18 mm in diameter.

Figure 20. Bedded tuffaceous siltstone of the Dismal Ashrock. Field of view approximately 20 x 15cm.

with minor beds of hematite-stained material (Fig. 20). The light colored beds are composed of either fine-grained calcite or microcrystalline quartz, whereas the grey beds are composed of a fine-grained (< 0.1 mm) assemblage of serpentine and opaque minerals.

Mafic Lava Flow

A 4 to 6 m thick mafic lava flow occurs directly above the komatiitic volcaniclastic unit and below komatiitic lapilli tuff. It constitutes <10% of the Dismal Ashrock. The flow is light to dark green, amygdaloidal, non-magnetic and typically pillowed (Fig. 21). The amygdules compose 10% of the rock and are radially oriented within the pillows. The pillows are elongate, plunge steeply to the south-west and range from 0.25 to 1 m in length and 0.25 to 0.5 m thick. In thin section the flow contains small (0.25-5 mm) skeletal crystals pseudomorphed by chlorite (15-40%), which are surrounded by chlorite (20-29%), calcite (5-10%), opaque minerals (1 - 5%), and hornblende (0-15%) with the remainder being optically unresolvable groundmass.

Komatiitic Volcanic Breccia

The komatiitic volcanic breccia is a small elliptical shaped unit 35 by 150 m that is found only in one locale near the top of the Dismal Ashrock. It consists of dark green-grey

Figure 21. Pillowed mafic flow from the Dismal Ashrock.

to grey-black, amygdaloidal, magnetic, juvenile lapilli that range in size from 1-6 cm. These fragments are directly analogous to the juvenile fragments in the komatiitic lapilli tuff except they are slightly larger in size. This unit also contains abundant (5-20% by volume) volcanic blocks (Fig. 22).

These blocks are sub-round, olive green, weakly to non-magnetic fragments that contain serpentine psuedomorphs after acicular crystals (olivine?) 0.5 mm in length. They are similar in mineralogy and textures to the cognate fragments in the komatiitic lapilli tuff, but, they are considerably larger (4-20 cm). Some of the blocks have rims that are composed of medium-grained (1-3 mm) green clinoamphibole and calcite.

One large, elongate, dark green mafic block 7 m in length was found that is non-magnetic, and consists of a medium-grained (<2 mm) assemblage of plagioclase (40%), green clinoamphibole (25%), chlorite (24%) and minor opaques and carbonate. The plagioclase occurs as well developed laths 1 to 2 mm in length and the rest of the minerals form finer-grained (<1 mm) interstitial material. Accidental fragments of carbonate are also found within this unit.

II.4 Alteration of the Dismal Ashrock

Three alteration types of the Dismal Ashrock occur in localized areas: pyrite, oxidized (red-brown) and Fe-depleted (pale grey or green).

Figure 22. A volcanic block from the volcanic breccia unit of the Dismal Ashrock. Coin is 24 mm in diameter.

The pyrite alteration type is found in discontinuous lenses throughout the Dismal Ashrock that may or may not be conformable with the bedding. They constitute <10% of the Dismal Ashrock. They are yellow and black, with a massive or fragmental appearance, and consist of pyrite with minor chert and carbonaceous material. The pyrite ranges from consolidated and resistant to unconsolidated and extremely friable. In addition, the pyrite is locally partially replaced by iron oxides such as goethite, hematite and limonite which are more resistant than the pyrite areas (Fig. 23).

The oxidized alteration type is red to brown, in color and primary textures are preserved. It is found in discontinuous patches near the contact with the underlying iron formation, with the alteration extending 20-30 m up into the Dismal Ashrock from joints and the basal contact (Fig. 24). This alteration type composes <5% of the Dismal Ashrock. In thin section this alteration type is seen to consist of a fine-grained (<.5 mm) mat of actinolite (35%), chlorite (30%), calcite (10%), opaque minerals [other than hematite] (12%), serpentine (10%), and hematite (3%) with the remainder being unresolvable and having an overall reddish-brown color.

The Fe-depleted alteration type is light green to very pale blue in color and is also found in discontinuous patches near the contact with the underlying iron formation. It composes <5% of the Dismal Ashrock. No spatial relationship

Figure 23. Pyrite alteration in the Dismal Ashrock that has been partially oxidized. Coin is 24 mm in diameter.

Figure 24. Oxidation alteration along a joint in the Dismal Ashrock. Coin is 24 mm in diameter.

between this type of alteration and the oxidized alteration was found. Primary fragmental and vesicular features are preserved. It consists of the following fine-grained (<0.1 mm) assemblage: calcite (23-35%), actinolite (28-30%), serpentine (13-20), chlorite (5-15%), opaques (9-10%) and quartz (2-7%). The matrix consists of calcite with minor quartz.

II.5 Stratigraphy of the Grassy Portage Bay Ultramafic Pyroclastic Rock Unit (GUP)

The Grassy Portage Bay ultramafic pyroclastic rock unit (GUP) occurs in an arcuate fold interference pattern of Ramsay type 3 (Plate 2). The GUP is in contact with Coutchiching sediments to the west and Keewatin mafic volcanics (sample 562a, Appendix II) and intrusive rocks to the east and north. The contact zones are poorly exposed, strongly foliated, and can contain intrafolial folds. The contacts are typically intruded by green to black mafic dikes consisting predominantly of a fine-grained (<0.5 mm), foliated assemblage of altered plagioclase and hornblende (samples 529 and 542a, Appendix I and II). The intrafolial folds are also present in the interior of the unit and are evidence for a high degree of deformation. For this reason no stratigraphic section has been determined. However, the GUP was divided lithologically into komatiitic lapilli tuff, which constitutes the majority of the unit, and komatiitic volcanic breccia which is found in only

one locality just north of Highway 11 (see Plate 2).

II.6 Description of the Lithologic Units of the GUP

Komatiitic Lapilli Tuff

The komatiitic lapilli tuff makes up over 90% of the GUP and in outcrop it appears as a fragmental, bright green to dark grey rock (Figs. 25, 26). The fragments range in size from 1 mm to 6 cm, are rounded to angular and are commonly amygdaloidal (up to 30%)(Fig. 27). The percentage of lapilli versus ash size fragments and matrix varies considerably and portions of this unit can be classified as ash tuff (less than 25% lapilli size fragments) or lapillistone (over 75% lapilli size fragments). Primary fragmental textures are easier to discern in the grey rocks. Cored lapilli are commonly found in the grey rocks and rare in the green ones (Fig. 28). Composite lapilli are rare in the grey rocks and have not been found in the green rocks (Fig. 29).

The variation in color is a reflection of the mineralogy. In thin section the dark grey komatiitic lapilli tuff contains a fine-grained (<0.1 mm) assemblage of tremolite (35-58%), chlorite (13-95%), opaque minerals (15-22%), and talc (0-30%). The fragments consist of fine-grained(<0.05 mm), colorless tremolite laths, chlorite plates and equant and elongate opaque minerals whereas the matrix and amygdules consist of coarser grained (0.5-.1mm) talc, actinolite and chlorite (Fig. 27).

Figure 25. Grey lapilli tuff from the GUP. Coin is 24 mm in diameter.

Figure 26. Green lapilli tuff from the GUP. Coin is 24 mm in diameter.

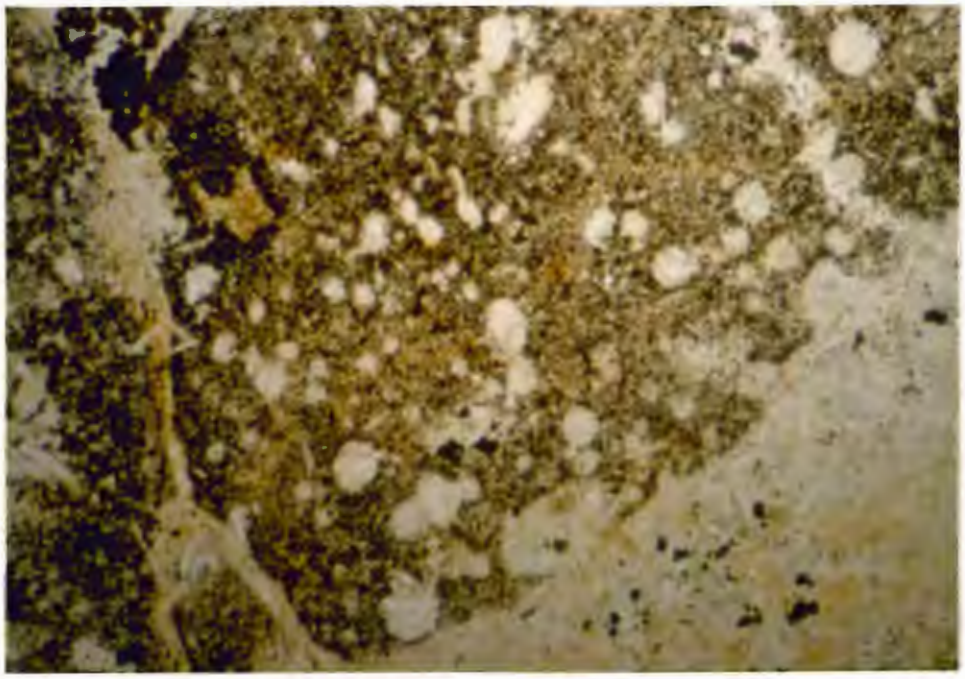

Figure 27. Photomicrograph of amygdaloidal pyroclast from a grey lapilli tuff of the GUP. The fragment consists of tremolite, chlorite, talc and opaque minerals whereas the matrix consists of talc, chlorite and tremolite. Plane polarized light, field of view 0.8 x 0.5 mm.

Figure 28. Cored lapillus from the GUP. Coin is 21 mm in diameter.

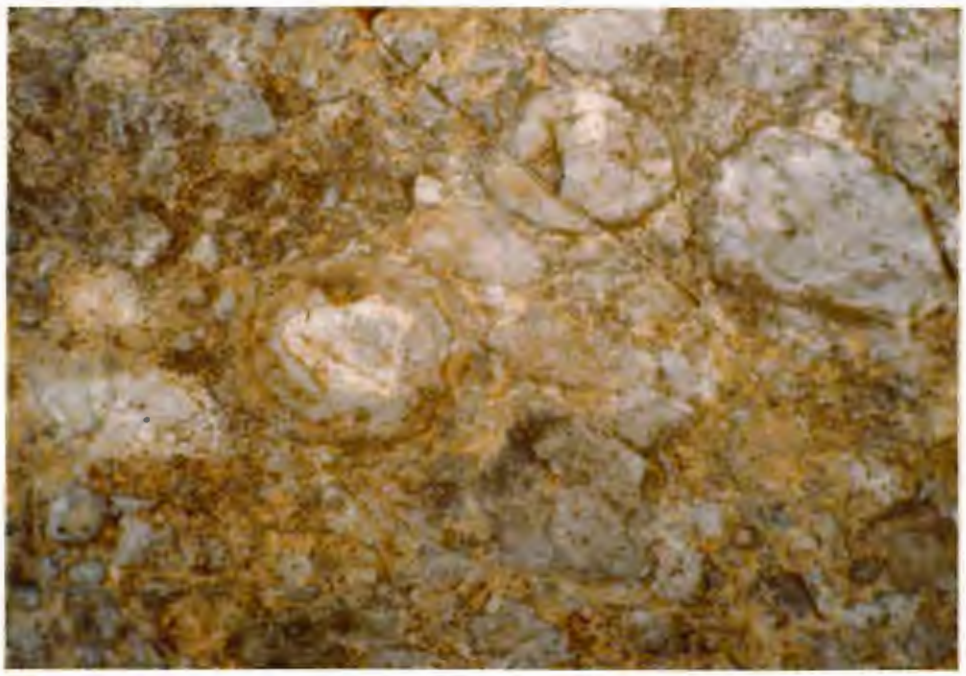

Figure 29. Cored and composite lapillus from the GUP. The cored lapilli (center, 3 cm in diameter) has two rims of quenched lava. The cored lapillus (top right center) consists of two smaller fragments in a rind of quenched lava.

The lapilli contain varying amounts (0 - 30%) of small (< 2 mm) amygdules (Fig. 27) which consist of tremolite, talc and chlorite.

Cognate fragments are found within the grey rocks and are olive green in color, angular, non-magnetic and weather out in negative relief compared to the surrounding juvenile fragments or rims if it forms the core of a cored lapilli (Fig. 28). They consist of a fine-grained (<0.1mm) assemblage of talc (70%), chlorite (13%), actinolite (13%) and opaque minerals (4%).

One accidental fragment of carbonate was found that was 20 cm long and elliptical in shape (Fig. 30). Mineralogically it consists of medium-grained (1-2 mm) calcite.

In thin section the bright green komatiitic lapilli tuff is more strongly recrystallized than the grey variety and fine-scale textures like vesicles are partially to totally destroyed. However, the fragments are visibly marked by an abrupt change in quantity and type of opaque minerals. The fragments contain over 15% of very fine-grained (<.1 mm) opaque minerals whereas the matrix consists of less than 5% coarser-grained (<.3 mm) opaque minerals. The green komatiitic lapilli tuffs have the following highly variable assemblage: actinolite-tremolite (0-43%), chlorite (20-26%), hornblende (0-50%), talc (0-20%), carbonates (2-5%), diopside (2-25%), opaque minerals (10-12%) and sphene (1-5%). The diopside usually

Figure 30. Accidental carbonate fragment in the GUP. Coin is 24 mm in diameter.

occurs as fine-grained (<.1 mm) granular grains concentrated in the matrix surrounding the fragments (Fig. 31).

Cognate fragments that are found within the green rock also have a green color and are angular in shape. They have the following fine-grained (<0.5 mm) mineral assemblage: hornblende (70%), chlorite (24%), sphene (5%) and opaques minerals (1%).

Komatiitic Volcanic Breccia

The komatiitic volcanic breccia occurs just north of Hwy 11 and outcrops over an area 40 by 250 m in size. It is dark grey, and consists of 5-20% volcanic bombs and blocks surrounded by lapilli which are similar to the lapilli in the grey komatiitic lapilli tuff (Fig. 32). The bombs are amygdaloidal with smooth surfaces whereas the blocks are angular and non-amygdaloidal.

In thin section this unit is very similar to the komatiitic lapilli tuff and has the following fine-grained (<0.5 mm) assemblage: tremolite (38-54%), chlorite (15-20%), opaque minerals (21-25%), and talc (10-17%). The matrix and amygdules contain talc, actinolite and chlorite.

II.7 Alteration of the GUP

A very limited portion (<5%) of the GUP is oxidized to a reddish brown color but retains well-preserved primary textures

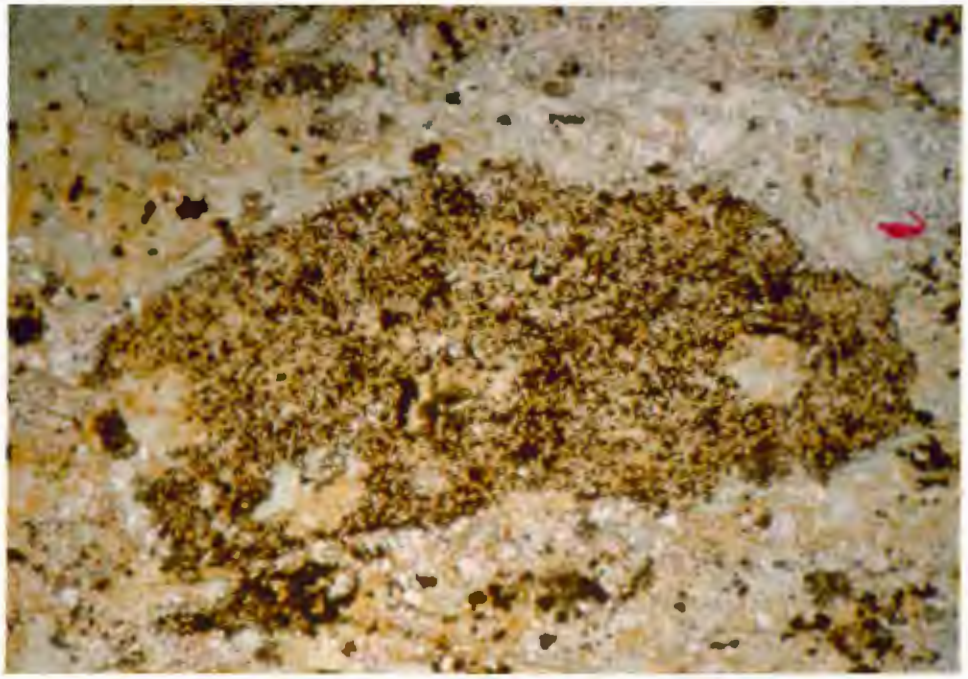

Figure 31. Photomicrograph of green lapilli tuff from the GUP. The fragment is composed of tremolite, chlorite and opaque minerals whereas the matrix consists of diopside, chlorite and sphene. Plane polarized light, field of view 0.8 x 0.5 mm.

Figure 32. Amygdaloidal volcanic bomb in tuff-breccia of the GUP. Coin is 24 mm in diameter.

such as fragments and vesicles. Samples from this oxidized rock consist of a fine-grained (<0.2 mm) assemblage of tremolite (40-58%), chlorite (15-20%), opaque minerals (20-22%), talc (5-10%) and amorphous unresolvable reddish brown material that stains the rock and is concentrated around the opaque minerals.

II.8 Summary of Physical Features

The Dismal Ashrock and the GUP both contain juvenile amygdaloidal pyroclastic fragments, including cored and composite lapilli. They both contain rock types that vary from ash tuffs to lapillistones to volcanic breccia. However, lapilli tuff is the predominant rock type in each unit. Both units contain cognate fragments of ultramafic character and accidental fragments of carbonate. The Dismal Ashrock also contains accidental tonalite fragments. In addition the Dismal Ashrock includes komatiitic volcaniclastic rocks and a mafic lava flow that are not found in the GUP.

The Dismal Ashrock is part of a supracrustal sequence that overlies an erosional unconformity whereas the contacts of the GUP are highly strained and the unit is deformed to such a degree that no primary relationships with its bordering units can be established.

The Dismal Ashrock consists of the following mineral assemblage: actinolite-tremolite, serpentine, chlorite, talc

and opaque minerals with or without a matrix consisting predominantly of carbonate. The GUP contains two distinct types of mineralogy. The grey rocks consist of tremolite, chlorite, talc and opaque minerals with the matrix consisting of talc, tremolite and chlorite. The green rocks consist of actinolite-tremolite, chlorite, hornblende, talc, diopside, opaque minerals, carbonates and sphene. The diopside is concentrated in the matrix surrounding the fragments. The Dismal Ashrock and the GUP have undergone greenschist and amphibolite facies metamorphism respectively. This difference in metamorphic grade is the major cause of the differences in mineralogy between the Dismal Ashrock and GUP.

The Dismal Ashrock contains three alteration types: Fe-enriched, Fe-depleted and Pyritized. The GUP contains only an Oxidation alteration type.

The physical character of the Dismal Ashrock and GUP indicate that explosive volcanic activity is responsible for their formation. The following section is an analysis of the evidence for, and the nature of, explosive volcanic activity in the production of the Dismal Ashrock and the GUP.

II.9 Volcanological Interpretation

Fragmental komatiitic rocks produced by explosive volcanism are rare on a global scale. They have been reported from Finland (Saverikko, 1983 and 1985), Australia (Nisbet and

Chinner, 1981), Quebec (Gelinas et al.,1976) and Columbia (Echeverria and Aitken, 1986). The Dismal Ashrock and the GUP are unique in this group for two reasons. First, they contain no ultramafic effusive rocks. Second, fragments from these units have a greater concentration of vesicles (up to 30% by volume) than reported for any other komatiites.

Fragmental komatiitic rocks can be produced by a number of mechanisms other than explosive volcanic activity. For example, erosion of pre-existing komatiites or passive quenching of subaqueously extruded komatiites could produce fragmental komatiitic rocks.

The komatiitic volcaniclastic rocks present in the Dismal Ashrock are witness to these types of processes. The interbedded ultramafic and quartz beds in these units indicate some type of sedimentary transport process in their development. In addition these volcaniclastic rocks and the mafic flow (in the Dismal Ashrock) indicate that the komatiitic lapilli tuff and volcanic breccia were not produced in one continuous eruption but rather the eruption was interrupted for "considerable" periods of time. The volcanism before and after the deposition of the volcaniclastic rocks has the same physical characteristics indicating that the same eruptive processes were operating but at different times.

The Dismal Ashrock and GUP contain cored and composite lapilli which require fragments of magma or accidental material

to be ejected and acquire a rind of magma either by transport through a magma aerosol in free space or as it leaves the magma body. To produce these types of fragments it is necessary to eject them from a melt and they are therefore unequivocal evidence of explosive volcanic activity. The explosive volcanic activity was likely to be phreatomagmatic as opposed to pure magmatic explosivity.

There are several lines of evidence that support phreatomagmatic activity in this case. First, the low viscosity of these magmas, inferred from their komatiitic composition, would make purely magmatic explosive activity very unlikely because their low strength could not easily confine high volatile pressures. Second, the vesicularity of the fragments ranges from 0 to 30%. This indicates that some other mechanism, other than exsolving volatiles, was driving the explosive activity. Third, pillowed mafic flows occur in the middle of the Dismal Ashrock indicating eruption into a subaqueous environment. Fourth, many juvenile fragments contain quench-textured crystals. For example, the small (5 mm) cored lapilli from the Dismal Ashrock has an outer rind of quenched magma 1 mm thick that contains skeletal and microspinifex crystals. This magma was not completely quenched to glass despite its very limited thickness, indicating that this fragment may not have been erupted directly into water but rather into superheated steam, either in an eruption cloud or

the conduit.

Therefore, it seems likely that phreatomagmatic activity was the cause of the explosive products in the Dismal Ashrock and GUP. Many komatiites show evidence for subaqueous extrusion (hyaloclastite, pillows and direct association with other subaqueous rocks) yet contain no evidence for explosive volcanic activity. Considering the global rarity of pyroclastic komatiites, the circumstances must be quite rare that enable komatiite magma to interact with water in an explosive manner.

Phreatomagmatic activity is controlled by the water/magma ratio (Fig. 33). For very high ratios (typical subaqueous eruptions) the water is not explosively expanded to steam. However, for subaqueous eruptions a number of mechanisms can increase the amount of magma in contact with the water thereby allowing for explosive expansion of steam. These are outlined below.

Phreatomagmatic activity can be classified as either contact surface steam explosivity and bulk interaction steam explosivity (Fig. 34) (Kokelaar, 1986). Contact steam explosivity describes the situation where the contact between water and magma occurs at the outer surface of the magma. In contrast, bulk interaction steam explosivity describes the situation where water is ingested by the magma or trapped close to it, usually by the magma engulfing sediments or admixing

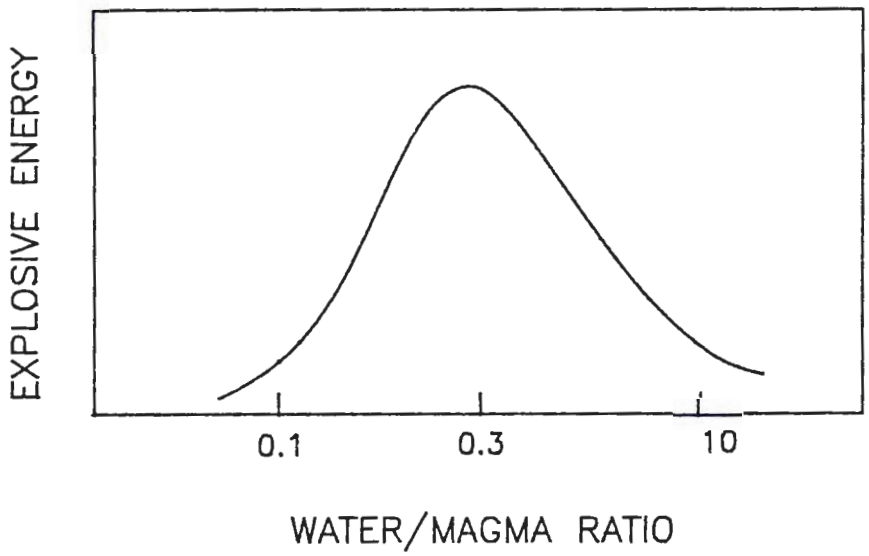

Figure 33. Explosive energy as a function of water/magma ratio (from Sheridan, 1983).

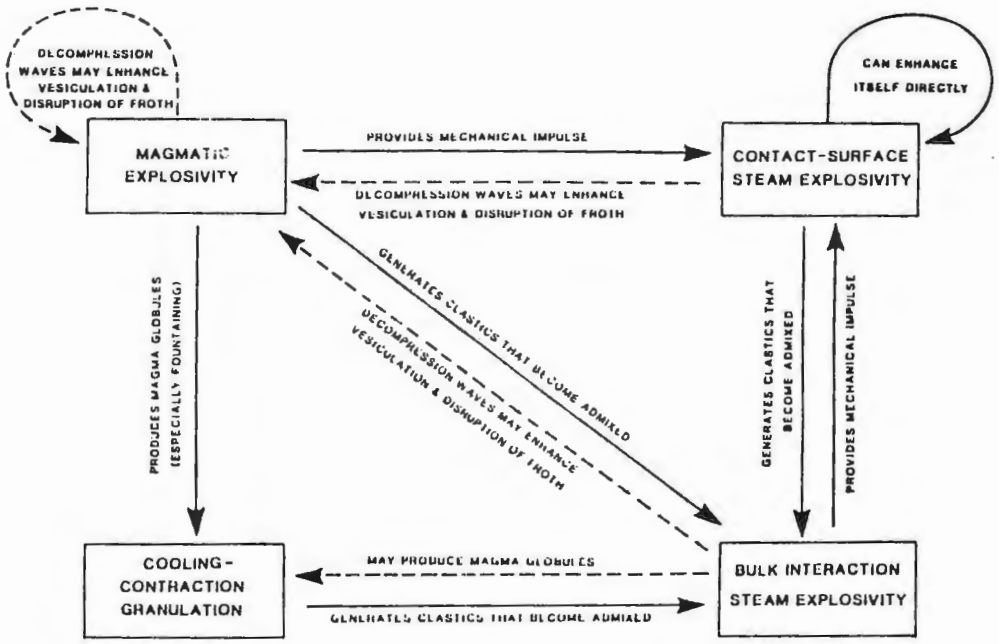

Figure 34. Classification of phreatomagmatic activity (from Kokelaar, 1986).

water and magma fragments after an eruption has begun.

Considerable quantities of sedimentary rock occur beneath the Dismal Ashrock. However, accidental fragments of these sedimentary rocks are rarely seen in the pyroclastic deposits of the Dismal Ashrock. It therefore, seems unlikely that bulk interaction steam explosivity occurred by ingesting these sediments. Water magma interaction probably occurred further up the conduit and that contact steam explosivity was the likely initial phase of explosive activity in the Dismal Ashrock.

Field evidence from recent basaltic eruptions indicates that a vigorous mechanical impulse (high velocity impact between water and magma), such as large, fast cascades of magma into water, is required to fragment the melt and start contact surface steam explosivity (Kokelaar, 1986). However, Wohletz (1986) has described two methods by which explosive magma water interaction has been generated without an "outside trigger" under labratory conditions. Both methods begin by the rapid and cyclic growth and collapse of steam films over the melt from spontaneous nucleation of steam. This can result in either 1) fluid instabilities or 2) pressure waves. The fluid instabilities increase the amount of surface area of melt in contact with water. Wolhletz believes that these types of interaction occur on only a very small (non-volcanic) scale. The pressure waves can fragment the melt and also increase the

surface area of melt in contact with water. This pressure wave is a trigger to fragment the melt and thereby allow increased water magma contact. However, both of these methods are unlikely initiating events for explosive komatiitic volcanism for the simple reason that if characteristics of typical komatiite magma water interaction were sufficient to generate explosive activity surely there would be more examples. It is therefore logical to assume that another factor, other than one inherent in typical komatiite-water contact, might be a requirement to initiate a phreatomagmatic eruptions in subaqueous komatiites (as is the case in recent mafic eruptions [Kokelaar, 1986]).

Both the Dismal Ashrock and the GUP are anomalously high in percentage of vesicles for komatiites. A vesiculating magma in the conduit could produce frothing, increased flow rate relative to the conduit width, and perhaps fire-fountaining (Wilson and Head, 1981). All of these processes could produce increased surface area and melt fragmentation allowing for intimate contact between water and magma and initiate steam explosions that could be self-fueling by constantly fragmenting more melt. Therefore, the volatiles and their resultant effects on the eruption characteristics in this magma are the likely initiating factor in producing the phreatomagmatic activity. The source of these volatiles will be discussed in the following chapter.

The komatiitic lapilli tuffs probably represent more distal deposits than the komatiitic volcanic breccia. The mafic flow is found only over komatiitic volcaniclastic rock, which most likely represents a primary topographic low. The lava flow probably originated from a volcanic center distal to that of the komatiitic pyroclastics and flowed into this topographic low.

III. GEOCHEMISTRY

III.1 Introduction

The purpose of this chapter to document and compare the compositions of the Dismal Ashrock and the GUP, and to determine the effects of alteration, the amount and type of matrix material, and assimilation on the composition of these units. Fifty-five samples, 32 from the Dismal Ashrock and 23 from the GUP (including four duplicates) were analyzed for major oxides and 11 trace elements. The analyses were done by XRAL of Toronto, and the results, along with the analytical methods employed are listed in Appendix II.

Summaries of major element and trace element data, calculated on a volatile-free basis, for the Dismal Ashrock and the GUP are presented in Tables 3 and 4 respectively. The data for the komatiitic lapilli tuff and volcanic breccia are presented together under the heading of komatiitic pyroclastic rocks. The Dismal Ashrock contains carbonate-rich matrix material, whereas the GUP's matrix material is predominantly talc, tremolite, chlorite and diopside. Therefore the data were calculated on a volatile free basis to facilitate comparison between these two units that have large variations in volatile content. Samples from the Dismal Ashrock have 0-30% matrix material consisting mainly of carbonate minerals.

Table 3. **Summary of major and trace element data for units within the Dismal Ashrock. All oxides are calculated volatile free.**

	Komatiitic pyroclastic rocks n=5		Komatiitic volcaniclastic rocks n=5		Mafic flow and block n=2	
	range	average	range	average	range	average
SiO2	41.08-45.69	43.80	33.96-49.61	42.75	49.37-51.21	50.29
TiO2	1.48- 1.90	1.66	0.36- 2.31	1.29	0.91- 0.98	0.94
Al2O3	4.48- 6.35	5.14	3.71- 7.48	5.76	14.21-15.41	14.81
Fe2O3	4.05- 6.97	5.24	4.34-25.06	12.26	2.47- 3.19	2.83
FeO	10.25-14.17	12.15	8.91-15.10	11.21	9.33- 9.64	9.49
MnO	0.26- 0.34	0.29	0.14- 0.66	0.39	0.22- 0.23	0.22
MgO	16.72-23.65	19.23	5.33-18.21	12.23	7.70- 9.24	8.47
CaO	4.59-15.70	9.62	0.36-23.80	12.40	6.22-10.19	8.20
Na2O	0.10- 0.63	0.33	0.00- 0.17	0.07	1.29- 4.62	2.95
K2O	0.03- 0.97	0.50	0.02- 0.16	0.07	0.22- 1.06	0.64
P2O5	0.10- 0.44	0.18	0.07- 0.17	0.12	0.07- 0.09	0.08
S	0.02- 0.05	0.04	0.02- 0.48	0.18	0.02- 0.04	0.03
Cr2O3	0.26- 0.33	0.29	0.07- 0.31	0.20	0.04- 0.05	0.05
NiO	0.15- 0.18	0.17	0.05- 0.22	0.13	0.02- 0.03	0.03
Total	98.52-98.84	98.64	98.13-99.68	99.08	98.63-99.46	99.04
H2O+	2.90- 4.90	3.72	2.60- 6.20	3.68	2.80- 4.10	3.45
CO2	0.50- 7.17	4.08	0.04-23.50	10.11	3.59- 4.49	4.04
LOI	6.23-11.94	9.56	5.21-26.77	14.66	7.73- 9.74	8.73
Ba	22- 121	67	0- 103	50	37- 291	164
Co	99- 120	108	46- 170	97	59- 72	66
Cr	1625-2035	1824	451-1770	1141	270- 301	285
Cu	210- 280	246	11- 490	240	140- 140	140
Ni	1100-1300	1200	310-1600	886	140- 250	195
Nb	14- 23	18	19- 38	25	0- 12	5
Rb	10- 44	22	15- 30	22	24- 37	31
Sr	36- 106	80	0- 164	32	75- 251	163
V	170- 230	192	120- 270	184	250- 260	255
Y	7- 12	9	3- 10	7	14- 15	15
Zr	54- 90	66	31- 95	59	18- 37	27

Table 4. **Summary of major and trace element data for the GUP. All oxides are calculated volatile free.**

	Grey komatiitic pyroclastics n=9		Green komatiitic pyroclastics n=4	
	range	average	range	average
SiO2	43.56-46.54	44.64	41.11-47.71	43.43
TiO2	1.47- 2.08	1.69	0.79- 1.30	1.13
Al2O3	3.70- 6.14	5.20	4.91- 8.65	6.32
Fe2O3	2.46- 8.55	6.77	3.38- 9.31	6.28
FeO	7.80- 9.67	9.10	10.36-14.74	12.18
MnO	0.24- 0.44	0.33	0.19- 0.25	0.20
MgO	19.39-23.91	21.79	10.96-15.09	13.36
CaO	2.45- 8.32	6.21	10.69-14.46	12.62
Na2O	0.13- 0.34	0.23	0.33- 0.78	0.54
K2O	0.02- 0.07	0.04	0.11- 0.36	0.21
P2O5	0.09- 0.15	0.12	0.02- 0.15	0.09
S	0.01- 0.09	0.04	0.01- 0.02	0.01
Cr2O3	0.17- 0.29	0.25	0.07- 0.23	0.19
NiO	0.07- 0.18	0.13	0.12- 0.17	0.14
Total	95.22-98.87	96.53	95.35-98.68	96.71
H2O+	2.60- 5.40	4.02	1.60- 3.50	2.28
CO2	0.00- 1.89	0.30	0.02- 0.15	0.07
LOI	3.00- 6.65	5.46	2.30- 4.36	3.26
Ba	45- 113	73	0- 87	39
Co	63- 110	82	79- 100	91
Cr	1135-1845	1639	485-1555	1265
Cu	22- 590	124	79- 100	27
Ni	560-1300	958	890-1300	1098
Nb	12- 52	28	14- 31	21
Rb	0- 23	7	0- 19	9
Sr	0- 62	22	0- 18	2
V	140- 240	172	130- 250	175
Y	9- 19	12	4- 12	8
Zr	58- 90	71	36- 53	21

This has resulted in large loss on ignition values (LOI). In contrast the GUP does not now have a carbonate matrix and therefore has considerably smaller LOI values.

The average and range for major oxides and trace elements for the komatiitic pyroclastic rocks, komatiitic volcaniclastic rocks, and mafic flows and blocks of the Dismal Ashrock are presented in Table 3. Only those samples with relatively low L.O.I. were used for these summaries and averages (<12.00 wt% for the komatiitic pyroclastic and mafic rocks and <27.00 wt% for the volcaniclastic rocks). An inspection of these data shows that the komatiitic pyroclastic rocks have low SiO_2 contents (41.08 - 45.69 wt%) and high MgO contents (16.72 - 23.65 %). In addition they have low Al_2O_3 concentrations (4.48 - 6.35 %). The komatiitic volcaniclastic rocks show similar characteristics but with greater variations in SiO_2 (33.96 - 49.61 %), MgO (5.33 - 18.21 %) and Al_2O_3 (3.71 - 7.48%) contents. The mafic flows and blocks have higher SiO_2 (49.37 - 51.21 %), Al_2O_3 (14.21 -15.41 %) and Na_2O (1.29 - 4.62 %) contents and lower MgO contents (7.62 - 9.15 %).

The average and range for the grey komatiitic pyroclastics and the green komatiitic lapilli tuffs of the GUP are presented in Table 4. An inspection of these data shows that the grey komatiitic pyroclastics also have a low SiO_2 content (43.56 - 46.54 %) and a high MgO content (19.39 - 23.91 %). Al_2O_3 concentrations range from 3.70 to 6.14 %. The green

komatiitic lapilli tuffs have a wide range of SiO_2 (41.11 - 47.71 %) and Al_2O_3 (4.91 - 8.65 %) concentrations, high CaO (10.69 - 14.46 %) and moderate MgO contents (10.96 - 15.09%). These are called low-MgO komatiitic rocks.

Analyses for mafic dikes from the Steep Rock Group and GUP are presented in Table 5. Alteration has affected the composition of some of the dikes. All of the dikes have higher Al_2O_3 values (>12.73 %) and lower Cr values (<680 ppm) than the pyroclastic deposits of the Dismal Ashrock and GUP. Therefore, these dikes could not be feeders for the pyroclastic rocks. The high-Mg mafic dikes from the Steep Rock Group (Table 2), described by Wilkes (1987) are higher in Al_2O_3 (avg. 7.91 %) and lower in TiO_2 (avg. 0.50 %) and $Fe_2O_3^*$ (avg. 10.30%) than the komatiitic pyroclastic rocks and are also unlikely feeders for the Dismal Ashrock.

Samples from the Dismal Ashrock and the GUP with small proportions of matrix material are compared to representative komatiitic samples and suites from Munro Township, Ontario; Barberton Mountain Land, South Africa; and a recently reported high Fe and Ti basaltic komatiite from Boston Creek, Ontario (Stone, Jensen, and Church, 1988)(Table 6). Upon inspection it is apparent that the komatiitic pyroclastic rocks from the Dismal Ashrock and from the GUP are similar to one another, with the exception of CO_2 content, and they are distinct from komatiitic rocks from other areas. Compared to other

Composition of dikes in the Steep Rock Group and GUP

	Steep Rock Group				GUP	
	SRE-84	SRE-62	SRE-217	SRE-8	SS-529	SS-542a
SiO2	52.14	51.99	38.65	42.37	43.87	48.68
TiO2	1.92	0.82	0.93	1.22	1.46	0.85
Al2O3	13.46	12.73	13.93	16.46	13.46	13.89
Fe2O3	1.40	4.38	7.03	4.34	3.53	1.67
FeO	14.03	2.70	10.16	18.57	13.46	9.98
MnO	0.24	0.15	0.33	0.18	0.26	0.21
MgO	4.91	6.04	14.06	15.46	6.78	7.17
CaO	8.44	9.08	11.67	0.61	13.56	12.86
NA2O	1.56	6.05	0.03	0.06	0.97	1.82
K2O	0.24	1.51	0.15	0.52	0.69	0.99
P2O5	0.15	0.64	0.94	0.11	0.10	0.07
S	0.02	0.51	0.03	0.01	0.01	0.01
Cr2O3	0.00	0.04	0.12	0.08	0.02	0.03
NiO	0.00	0.03	0.45	0.06	0.02	0.01
Total	98.53	96.66	98.47	100.05	98.18	98.25
H2O+	4.40	1.10	6.10	8.40	1.60	1.80
CO2	6.91	5.70	12.20	0.28	0.09	0.03
LOI	12.17	7.05	20.00	10.09	2.62	2.78
Ba	30	16400	105	89	170	235
Co	58	40	170	96	67	57
Cr	28	269	680	468	129	178
Cu	110	51	140	34	14	28
Ni	32	200	2800	420	120	110
Nb	20	14	21	19	-3	11
Rb	10	32	-10	25	22	40
Sr	47	1100	506	-10	277	110
V	400	120	140	280	410	350
Y	27	21	25	5	10	17
Zr	76	122	121	74	21	25

Table 5. **Analyses of dikes from the Steep Rock Group and the GUP. All oxides calculated volatile free.**

Table 6. Chemical data for selected samples from the Dismal Ashrock and GUP compared to representative samples from Barberton, South Africa, Munro Township Ontario and Boston Creek Ontario.

sre-70	Ash tuff from Dismal Ashrock
sre-65	Lapilli tuff from the Dismal Ashrock
sre-91	Mafic flow from the Dismal Ashrock
ss-518	Grey lapilli tuff from the GUP
ss-581	Grey lapilli tuff from the GUP
ss-528	Green lapilli tuff from the GUP
BPK	Komatiite from Barberton Mountain Land (Nisbet and Sun, 1976).
MPK	Komatiites from Munro Township (Arndt and Nesbitt, 1982).
MBK	Basaltic komatiites from Munro Township (Arndt and Nesbitt, 1982).
BC	Basaltic komatiites from Boston Creek (Stone et al., 1987).

	Dismal Ashrock			GUP						
	SRE-70	SRE-65	SRE-91	SS-518	SS-581	SS-528	BPK n=1	MPK n=3	MBK n=4	BC n=3
SiO2	45.69	44.44	51.21	44.52	45.26	47.71	45.23	45.58	48.32	49.20
TiO2	1.61	1.50	0.91	1.77	1.62	1.30	0.20	0.40	0.57	1.14
Al2O3	4.79	4.59	15.41	5.82	3.70	6.51	3.66	8.91	11.41	6.70
Fe2O3	6.97	5.07	2.47	7.88	8.55	3.38				5.17
FeO	10.25	11.66	9.64	9.82	8.45	14.74				12.49
Fe2O3t	18.36	18.04	13.19	18.79	17.94	19.76	12.20	12.54	13.34	19.05
MnO	0.28	0.31	0.23	0.32	0.38	0.25	0.22	0.23	0.21	0.23
MgO	19.85	17.82	7.70	22.63	19.61	10.96	32.16	22.39	14.65	10.57
CaO	7.75	11.55	10.19	5.38	8.32	12.29	5.28	9.46	9.84	13.21
Na2O	0.25	0.26	1.29	0.13	0.34	0.78	0.44	0.64	1.26	1.44
K2O	0.51	0.74	0.22	0.07	0.03	0.36	0.17	0.09	0.07	0.07
P2O5	0.13	0.10	0.07	0.13	0.09	0.05	0.02	0.02	0.05	0.08
Total	98.08	98.04	99.34	98.47	96.35	98.33	101.11	100.27	99.71	100.28
LOI	6.23	8.95	9.74	6.25	3.98	2.30	6.31	4.41	3.66	2.94
Ba	81	55	37	78	82	41	11	11	19	87
Co	120	110	59	82	77	92	108	92		86
Cr	1900	1620	270	1700	1725	1545	3190	3333	1479	485
Ni	1200	1300	140	880	750	890	1931	894	350	535
Nb	16	17	12	27	27	22	1	1	1	0
Rb	31	25	24	23	10	12	4	3	2	1
S	500	500	700	200	200	100	80	223	0	2739
Sr	36	75	75	24	45	18	31	20	46	181
V	170	180	260	180	160	250	92	170	221	284
Y	12	9	14	14	12	10	3	11	14	12
Zr	70	58	18	77	60	53	9.6	20	28	33

komatiitic rocks, discounting those from Boston Creek, the Dismal Ashrock and the GUP are enriched in TiO_2, $Fe_2O_3^*$ (total Fe), MnO, P_2O_5, Ba, Nb, Rb, Sr, and Zr. In addition they have lower Cr (1135 - 2035 ppm) than other komatiites for equivalent silica and MgO concentrations. The average silica content for the Dismal Ashrock and GUP is low due in part to matrix material that is low in silica. However, even those samples from the Dismal Ashrock with no carbonate matrix have a low silica content(i.e. 45.16 wt% for sample SRE 70) and are as low or lower in SiO_2 content than those samples from Munro Township and Barberton.

Compared to the recently reported Fe-rich basaltic komatiites from Boston Creek, Ontario (Stone et al., 1988) the komatiitic pyroclastic rocks of the Dismal Ashrock and GUP are enriched in TiO_2, MnO, Cr, Ni, Nb, Rb, and Zr. They are relatively depleted in SiO_2, CaO, Na_2O, and Sr.

The Dismal Ashrock and the GUP form a tight cluster on the boundary between peridotitic and basaltic komatiite when plotted on a Jensen AFM diagram (Jensen, 1976)(Fig. 35). The low-MgO komatiites (green) from the GUP plot within the basaltic komatiite field. The Dismal Ashrock and the grey GUP plot in the same area when plotted on a MgO vs. Al_2O_3 diagram (Fig. 36). They are depleted in Al_2O_3 content relative to the Munro komatiites and Minnesota Fe-rich komatiites.

An Al_2O_3 vs. $FeO^*/(FeO^*+MgO)$ plot has been used to

Figure 35. A Jensen Cation plot (Jensen, 1976) comparing the composition of the Dismal Ashrock and the GUP with komatiites from Munro Township (Fred's Flow), Vermilion greenstone belt of Minnesota, Barberton Mountain Land, and high Fe and Ti komatiites of Boston Creek. Dike analyses of Table 2 and 5 are presented as triangles with accompanying abbreviations. The abbreviations and corresponding samples are as follows:

s1 = SRE 8
s2 = SRE 62
s3 = SRE 84
s4 = SRE 217
s5 = High-Mg dikes (Wilkes)
s6 = Mafic dikes (Wilkes)

g1 = SS 529
g2 = ss 542a

Data sources: Arndt et al. (1977), Jahn et al. (1982), Green and Schulz (1977) Schulz (1982) and Stone et al. (1987).

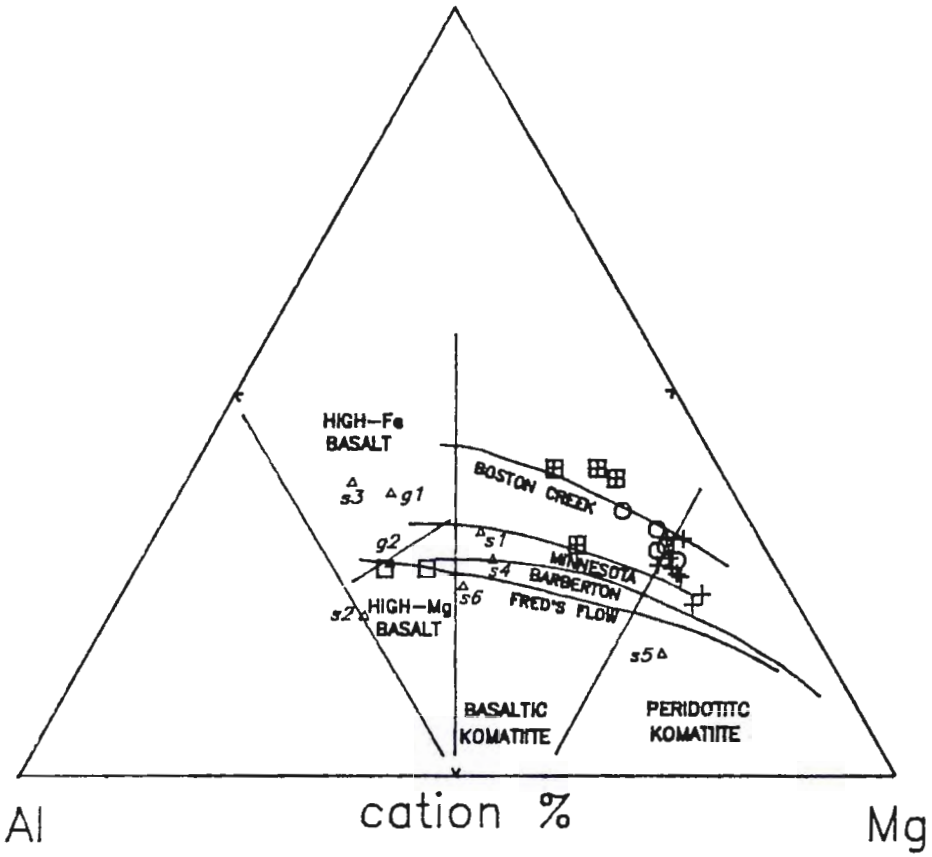

DISMAL ASHROCK

o Komatiitic pyroclastics
□ Mafic flow and block

GUP

\+ Grey komatiitic pyroclastics
⊞ Green komatiitic pyroclastics

▵ Dikes

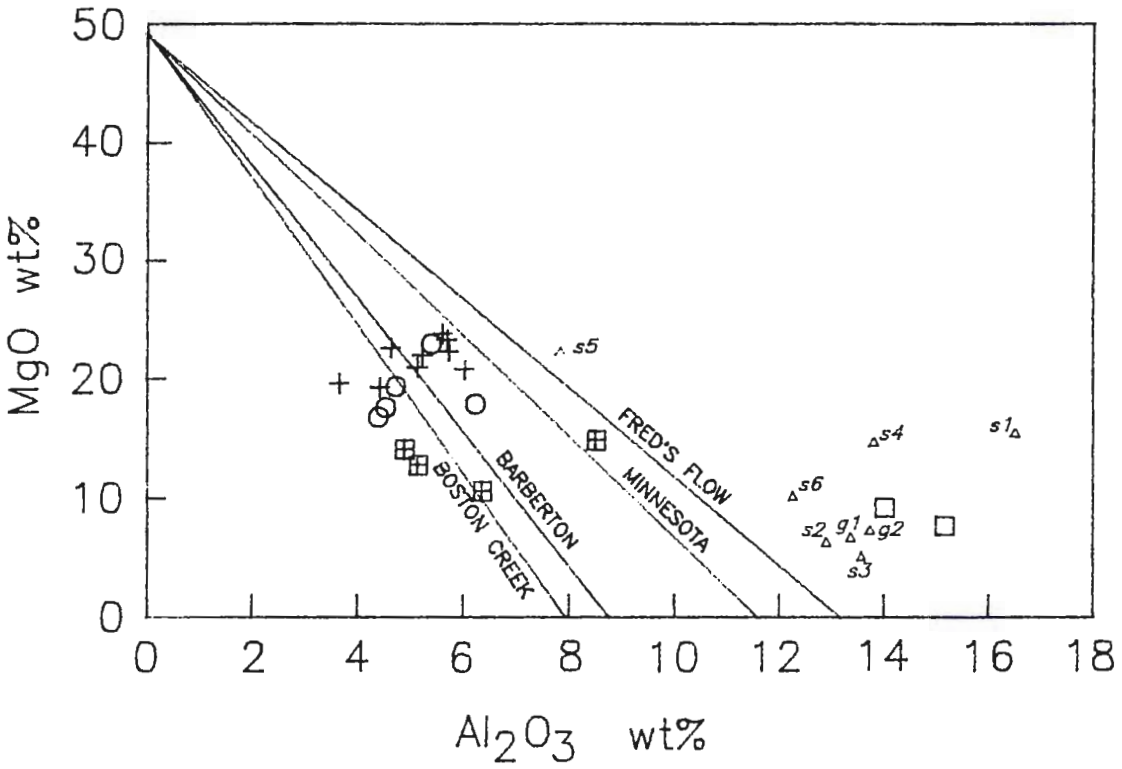

Figure 36. **A variation diagram for MgO versus Al_2O_3 for the Dismal Ashrock and the GUP relative to ratio lines of other komatiitic suites. Symbols and data sources as in Figure 35.**

distinguish Munro Township komatiites from tholeiites (Arndt, Naldrett and Pyke, 1977). This plot shows the Fe-enriched nature of the Dismal Ashrock and GUP relative to other komatiites (Fig. 37).

Stone et al. (1987) used a CaO/Al_2O_3 vs Al_2O_3/TiO_2 plot to distinguish Boston Creek komatiites from other komatiites. The Dismal Ashrock and the GUP have some of the same unusual chemical parameters as those of the Boston Creek komatiites (Fig. 38). However, the high CaO/Al_2O_3 ratio is due in part to carbonate matrix material high in CaO that has been added to the whole rock composition. In contrast the low Al_2O_3/TiO_2 values are not affected by matrix material and probably accurately represent the primary magma.

Komatiites typically have chondritic Ti/Zr ratios of 102 (Nesbitt and Sun, 1976). The Dismal Ashrock and the GUP have high Ti/Zr values, similar to those of the Boston Creek Basaltic komatiites (Fig. 39), however, the Dismal Ashrock and GUP have much higher absolute values of both Zr and Ti. These values are also much higher than the associated basalt flow.

The detailed stratigraphic column for a portion of the Dismal Ashrock is presented in Figure 40 showing the variation in concentration of selected elements. It is apparent that the mafic flow does not share the unique chemical characteristics of the komatiitic pyroclastic rocks and the komatiitic volcaniclastic rocks. It is also clear that after the short

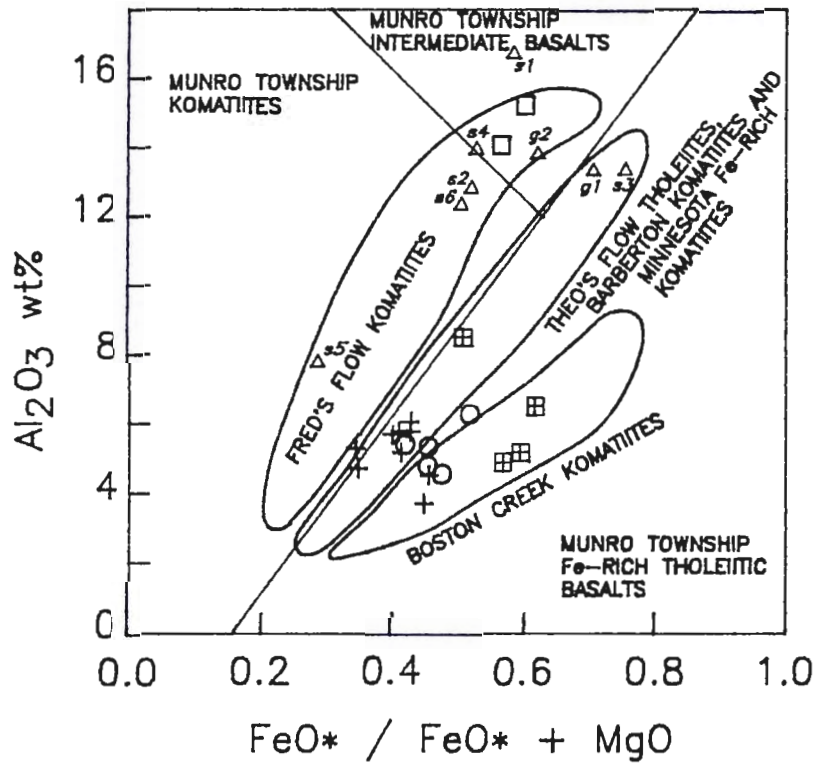

Figure 37. A plot of Al_2O_3 versus $FeO^* / (FeO^* + MgO)$ for the Dismal Ashrock and the GUP relative to other komatiitic suites. Symbols as in figure 35. Data sources Arth et al. (1977) and as in Figure 37.

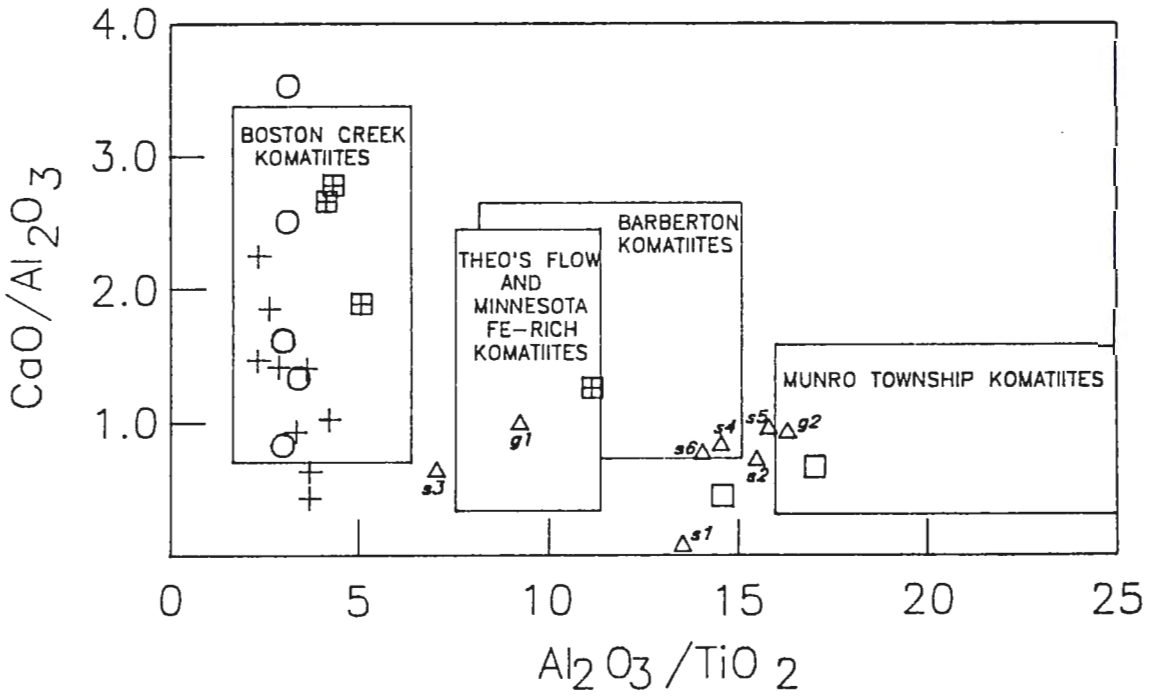

Figure 38. **A plot of CaO/Al_2O_3 vs. Al_2O_3/TiO_2 for the Dismal Ashrock, GUP and other komatiites. Symbols and data sources as in Figure 35.**

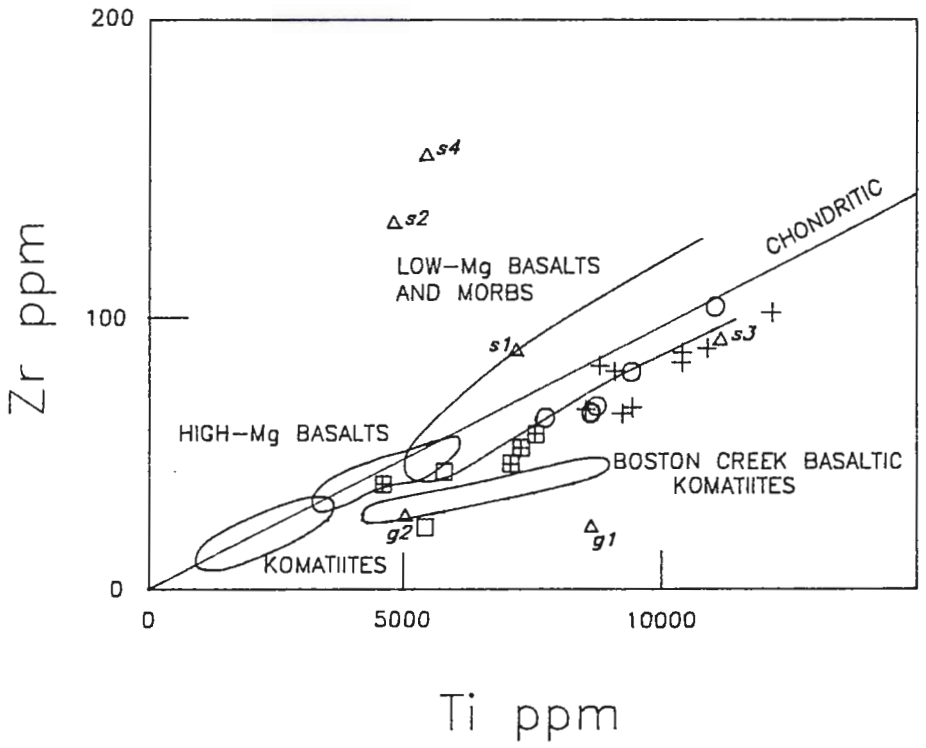

Figure 39. **A plot of Zr versus Ti for the Dismal Ashrock and GUP relative to typical komatiites and the Boston Creek Komatiites. Symbols as in Figure 35. Data sources: Arndt and Nesbitt (1982), Nesbitt and Sun (1976) and Stone et al. (1986).**

Figure 40. Detailed stratigraphic column for the Dismal Ashrock with variations in selected elements and Mg#.

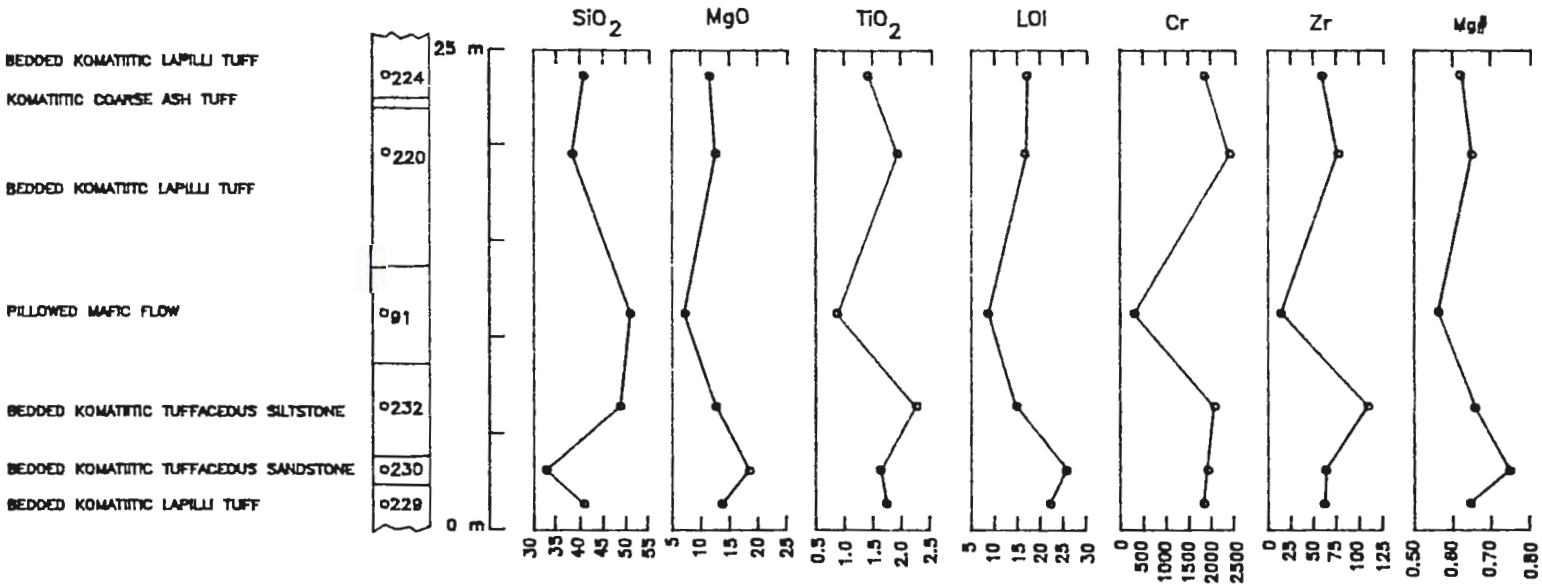

interlude of mafic volcanism the komatiitic volcanism returned with its unique chemical composition. Note the high LOI values due to carbonate matrix in the fragmental rocks.

It is extremely important to determine if the unique composition of these rocks is due to a primary melt from an enriched mantle or is the result of some other process. Therefore, alteration, including effects of matrix material and assimilation will be looked at in detail to determine if they are possible causes of the unique chemistry of the Dismal Ashrock and the GUP.

III.2 Alteration

Dismal Ashrock

The unique geochemical characteristics of the komatiitic units in the Dismal Ashrock are unlikely to be effects of alteration. The mafic flow, blocks and dikes within the komatiitic pyroclastics show no enrichment of TiO_2, K_2O, P_2O_5, Ba, Nb, Sr or Zr. It is very unlikely that alteration would enrich the ultramafic rocks in these elements and have no effect on the mafic rocks within them. Furthermore, the alteration zones within the Dismal Ashrock are of limited spatial extent, and the unusual geochemistry is common to both altered and unaltered zones. However, analysis of the alteration zones is useful in determining the relative mobility of the elements during alteration. One can assume that those

elements that were immobile in the alteration zones were also immobile outside of those zones.

The Dismal Ashrock has three alteration types of limited areal extent consisting of 1) oxidized, 2) iron- depleted and 3) pyritized. To determine the nature of the alteration types, excluding the pyrite alteration, the isocon method can be used (Grant, 1986). The isocon method uses a graphical plot of elements from an altered rock plotted against those of a least altered equivalent. Those elements that fall on a straight line represent those elements that are immobile. The isocon can be drawn through assumed immobile elements (in this case Al_2O_3). Those elements that plot with a steeper slope than the isocon have been gained in the alteration and those with a shallower slope have been lost, and those that plot with the same slope as the isocon have been immobile.

A sample from an oxidized zone plotted against a least-altered equivalent with an isocon drawn through Al_2O_3 is shown in Figure 41a. The alteration has increased the amount of CO_2, CaO, H_2O+, Fe_2O_3, Sr and Nb. There has been a loss of Na_2O, Rb, K_2O, MgO, SiO_2, Ba, Y and FeO. There has been no significant movement of $Fe_2O_3^*$, P_2O_5, TiO_2, MnO, Cr, Zr, Ni, Co and V.

The isocon diagram for an Fe-depleted sample with an isocon drawn through Al_2O_3 is presented in Figure 41b. This alteration has produced a gain in CO_2, CaO, SiO_2, Nb and V; and a loss of Na_2O, MgO, Fe_2O_3, FeO, P_2O_5, H_2O+, Sr and Ni. There

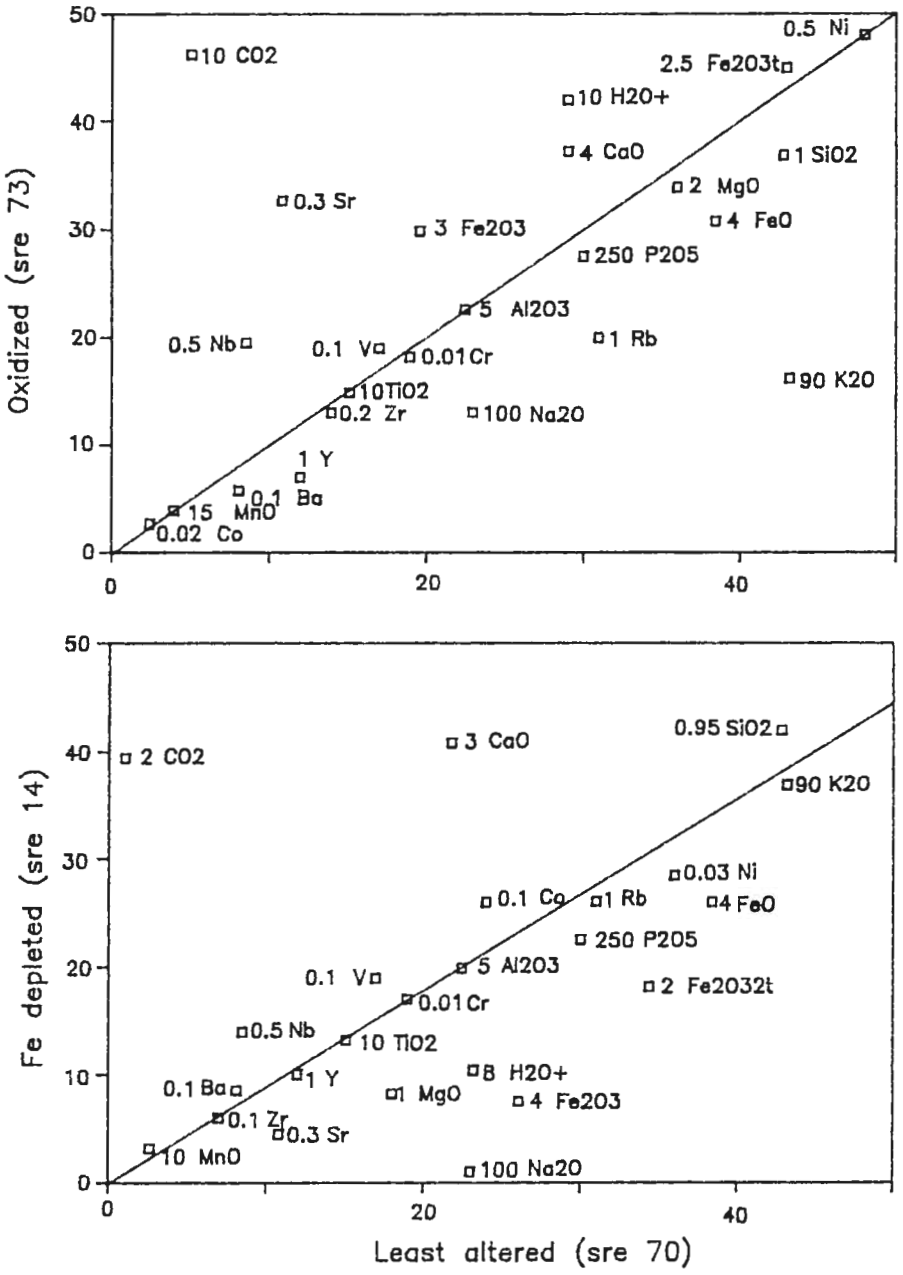

Figure 41. Isocon diagram for alteration zones in the Dismal Ashrock.
a) [top] Isocon diagram of an oxidized sample versus a least-altered sample.
b) [bottom] Isocon diagram of an Fe-depleted sample versus a least-altered sample.

has been no significant movement in Zr, Y, TiO_2, K_2O, Rb and Cr. In this case the least altered sample has more water than the altered sample. This apparently is due to the loss of MgO and gain of SiO_2 (quartz) in the altered sample inhibiting later formation of hydrous phases.

Outside of the alteration zones most of the komatiitic pyroclastic rocks have calcite as a matrix material, although two samples have dolomite as matrix material. An isocon diagram of a komatiitic lapilli tuff with calcite matrix versus a komatiitic ash tuff with virtually no matrix material shows that CO_2 and CaO have been added and have essentially diluted the primary rock chemistry with these elements (Fig. 42a). This addition of matrix material accounts for the low silica contents in samples with high CO_2 and CaO contents. No other elements have been highly mobile except for Na_2O and Sr which were gained and K_2O and Ba which were lost. This indicates that the samples with no carbonate matrix material (ie SRE 70 in table 3) may approximate the chemical composition of the magma at the time of the eruption.

An isocon for a sample with a ferroan (?) dolomite matrix shows the same pattern indicating that the CaO and CO_2 were introduced and the MgO was supplied from the rock (Fig. 42b). However, there is an addition of FeO which is probably in the dolomite structure. This matrix is very limited in distribution; it was only found in two samples. Therefore,

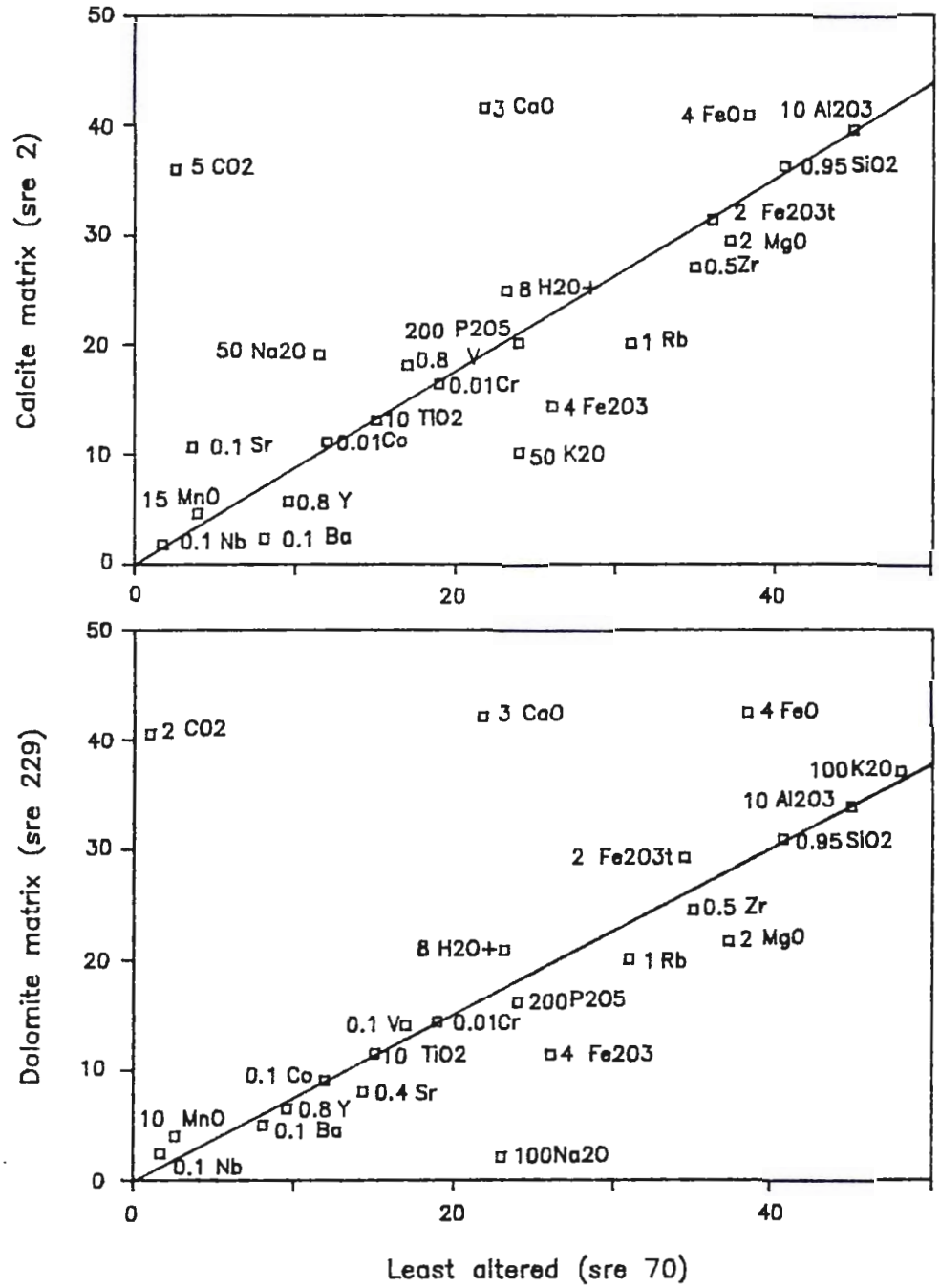

Figure 42. Isocon diagrams for samples from the Dismal Ashrock containing carbonate matrix.
a) [top] Isocon diagram of a sample from the Dismal Ashrock with a calcite matrix versus a sample with little carbonate matrix.
b) [bottom] Isocon diagram of a sample from the Dismal Ashrock with a dolomite matrix versus a sample with little carbonate matrix.

this matrix is not the source of high Fe values in the Dismal Ashrock.

Some generalizations can be made about the alteration of the Dismal Ashrock. First, TiO_2, Zr, Cr and Ni have been immobile during alteration and their high values are not the result of an alteration process. Second, the calcite matrix has added CaO and CO_2 whereas most other elements have been immobile. Therefore, the unique characteristics of the Dismal Ashrock represented in samples low in matrix material are concluded to approximate the chemical composition of the magma at the time of eruption.

Grassy Portage Bay Ultramafic pyroclastic (GUP)

An isocon diagram is presented in Figure 43 for a sample from the oxidized (brown) alteration zone plotted against a least-altered equivalent with an isocon drawn through Al_2O_3. It appears that H_2O+, Fe_2O_3, Fe2O3t, MgO, Rb, Co, Ni, Cr, Ba and Sr have been gained and K_2O, Na_2O, CaO, Y, V and Nb have been lost. The following elements appear to have little mobility: Zr, TiO_2, P_2O_5, and MnO.

The GUP has matrix material consisting of talc, tremolite, chlorite and diopside. The presence of diopside indicates a matrix richer in CaO than the pyroclasts. This matrix material might represent CaO rich carbonate that has reacted with the ultramafic rock fragments during metamorphism

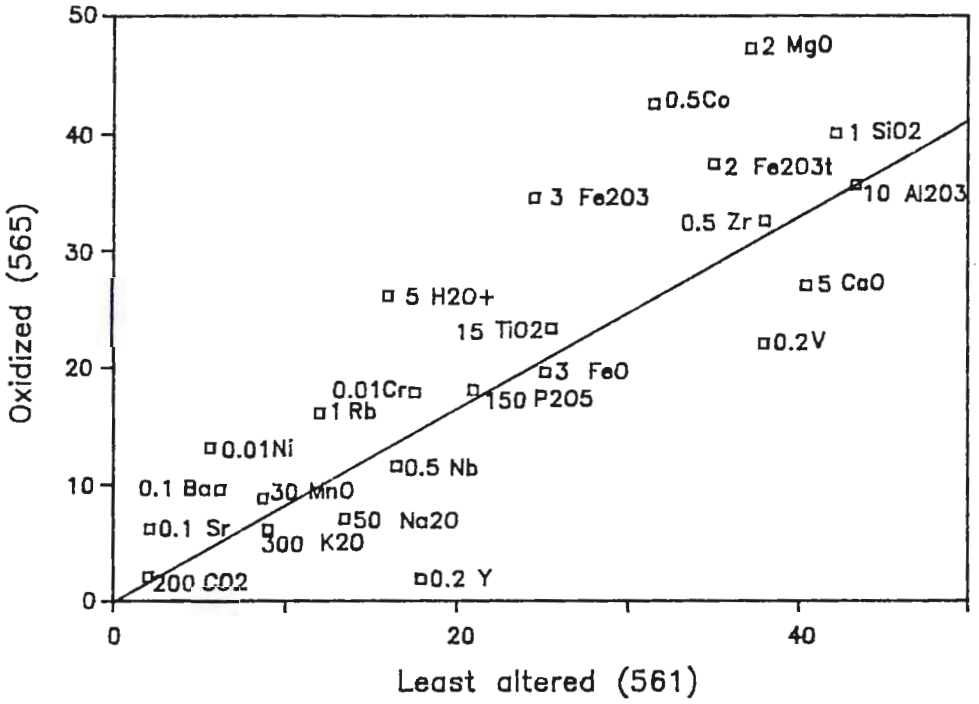

Figure 43. **Isocon diagram of an oxidized sample from the GUP versus a least altered sample.**

and liberated CO_2. This would have resulted in a dilution of the whole rock composition with CaO.

The alteration in the GUP is very limited in areal extent and Zr and TiO_2 have not been mobile in these zones. The composition of the unaltered samples with high SiO_2 and Cr (representing minor effects of matrix material) of the GUP is assumed to roughly approximate the magma composition at the time of its eruption.

III.3 Assimilation

Assimilation might have played a role in producing the unique chemical composition of these units. Recent work by Huppert and Sparks (1985a, 1985b) has shown that the low viscosity of komatiites results in turbulent flow (Fig. 44). This turbulent flow prohibits a chill margin from developing by constantly bringing hot magma into contact with wall rock which could results in large amounts of assimilation of wall rock. Huppert and Sparks (1985a, 1985b) have numerically modelled komatiite magma flow up through the crust and have determined that contamination by up to 25% sialic crust is possible as well as melting rates on the order of meters per day for dike walls (Fig. 45).

The Dismal Ashrock is the top unit in a supracrustal sequence that unconformably overlies a tonalitic gneiss basement. Accidental carbonate fragments of tonalite and

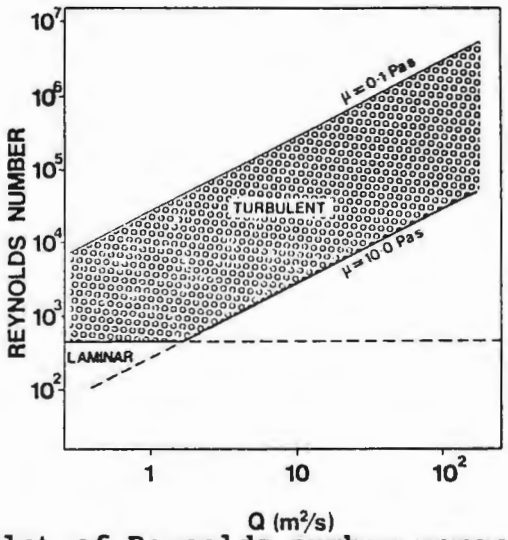

Figure 44. A plot of Reynolds number versus the two dimensional flow rate Q. The two diagonal lines represent the range in viscosity for komatiites. Komatiite magma flow will be turbulent in the field above the dashed line (from Huppert and Sparks, 1985a).

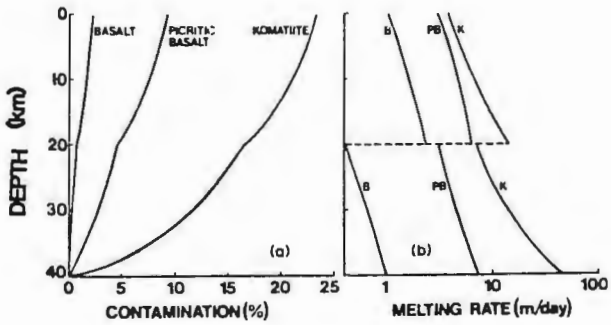

Figure 45. a) Variation in contamination with depth for three magma types that flow at a two dimensional flow rate (Q) of 25m^2/s.
b) Melting rate in meters/day as a function of depth. (From Huppert and Sparks, 1985b).
(dashed line divides assumed melting temperatures of 1000° above and 1200° below)

carbonate indicate that the magma moved up through these underlying units. Therefore, it seems possible that some aspects of the Dismal Ashrock's and the GUP's chemical composition (if it is correlative to the Dismal Ashrock and displaced tectonically) is due to assimilation of these materials.

REE data for the Dismal Ashrock (D. Stone pers. comm., 1989) show strong LREE enrichment in contrast to typical komatiites that have relatively flat REE curves or LREE depletion in the range of 5 to 10 times that of chondrites (Fig. 46). The Dismal Ashrock's REE pattern approximately mimics that of Archean tonalitic gneisses and the weathering products of the tonalitic gneiss directly below the Steep Rock Group and its absolute REE content is at a level between that of Archean tonalitic gneisses and typical komatiites. However, rocks produced from enriched mantle sources, i.e. alkalic basalts, are also enriched in LREE (Wilson, 1989).

By subtracting a component of sialic crust from a representative sample from the Dismal Ashrock (SRE 70) an assimilation model can be tested. Major and selected trace elements from a sample representative of the magma composition of the Dismal Ashrock (no carbonate matrix) and the average of 64 tonalitic gneisses from the Superior Province of the Canadian Shield are listed in Table 7. Also listed are the predicted primary magma if assimilation of 10 and 20% of

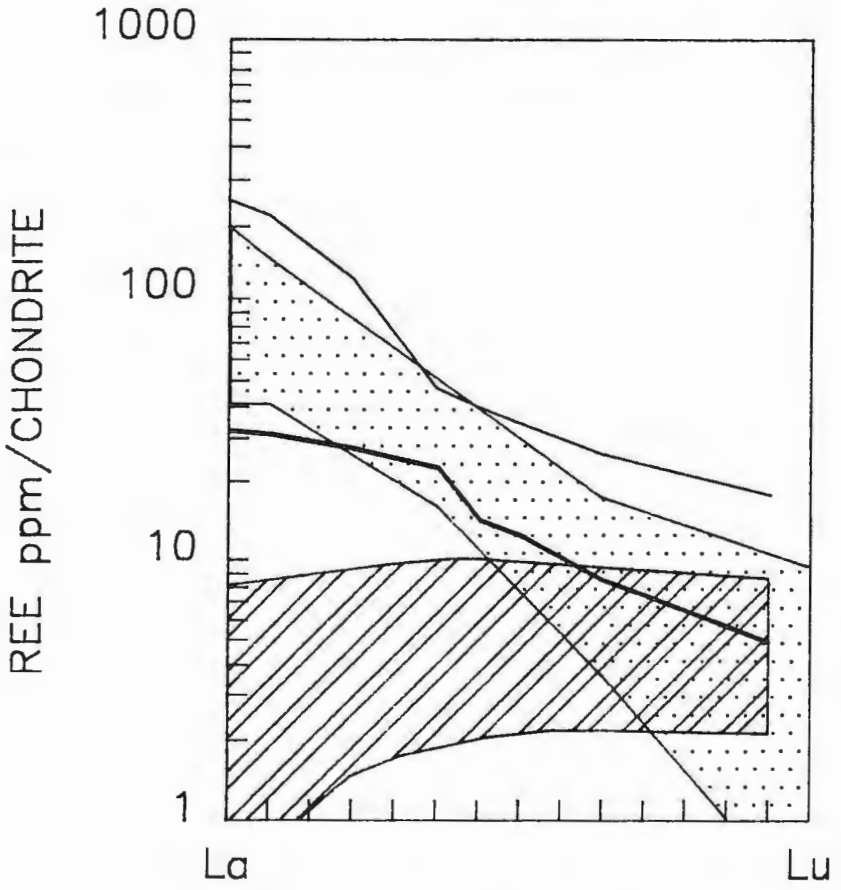

Figure 46. **A plot of REE values from the Dismal Ashrock (solid lower line), weathering product of the Marmion tonalite (solid upper line), range for Munro komatiites (diagonal ruled), and Archean tonalitic gneisses (dots). Data sources: Arndt and Nesbitt (1982), Arth et al. (1979), Collerson and Bridgewater (1979), and D. Stone pers comm. (1989).**

Table 7

	DA	Tonalite	P10	P20
SiO2	46.58	67.12	44.30	41.45
Al2O3	4.89	16.88	3.56	1.89
TiO2	1.64	0.43	1.77	1.94
Fe2O3	7.11	1.60	7.72	8.48
FeO	10.45	2.40	11.34	12.46
MnO	0.28	0.06	0.30	0.33
MgO	20.25	1.40	22.34	24.96
CaO	7.90	3.40	8.40	9.03
Na2O	0.25	4.59	-0.24	-0.84
K2O	0.53	2.00	0.36	0.16
P2O5	0.13	0.13	0.13	0.14
Total	100	100	100	100
Sr	38	416	-4	-57
Rb	33	55	31	27
Ba	85	526	36	-25
Zr	74	227	57	36
V	179	75	191	205
Cr	2005	17	2226	2502
Ni	1266	10	1406	1580

Table 7. **Predicted primary magmas (P10 and P20) if the Dismal Ashrock (DA [sample sre-70]) resulted from 10% and 20% of tonalite contamination. Tonalite composition is the average of Superior Province tonalites from Ermanovics, McRitchie and Houston (1979).**

tonalitic crust took place. The predicted primary magma assuming 20% contamination has only 41.45 wt% SiO_2 , which is not a reasonable primary magma (see Table 4), yet is still greater in Zr and Rb than other komatiitic rocks (compare with Table 6). K_2O levels are at a normal level in the predicted primary magma. However, the greatest enrichment in the contaminated magma would have occurred with Na_2O - the Dismal Ashrock and the GUP are depleted in Na20 with respect to other komatiites. Furthermore there should have been greater enrichment in Sr and Ba (the predicted primary magmas contain negative amounts of these elements). In addition, this model does not explain the enrichment of total Fe, TiO_2, P_2O_5.

Underneath the Dismal Ashrock are units rich in Fe and CO_2. To test if these units could be the source of Fe and volatiles (CO_2), detailed calculations can be carried out because the thickness of the layers and concentration of these components are known. The amount of these components added to the magma can approximately be determined by using Huppert and Sparks (1985) model of melting rates for material underneath komatiite flows (as an approximation for dike wall melting rates) and their model for flow rate through dikes (Fig. 47) The following calculations are based on a hypothetical $1m^3$ block of magma moving up through a dike. The amount of assimilation of a component is determined by dike width, flow rate (vertical velocity), thickness of unit, melting rate,

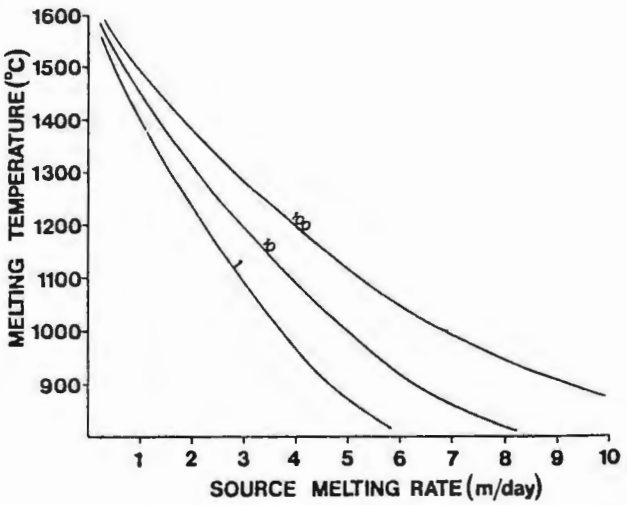

Figure 47. Variation in melting rate of material underlying a komatiite lava flow as a function of its melting temperature and the flow rate (represented by three lines at flow rates of 1, 10 and 100 m^2/s) of the komatiite lava (from Huppert and Sparks, 1985a).

concentration of component in melted rock and density of the rock according the following formula (the variables and constants are listed below):

M = melting rate for each dike wall

D = Dike width

V = vertical velocity (dependent on dike width)

C = concentration of component in wall rock

dw= density of wall rock (approximate)

T = thickness of sedimentary package

S = surface area of $1m^3$ of magma in contact with both dike walls (dependent on dike width)

mc= mass of a component added to magma

mk= mass of $1m^3$ of magma (assumed $2.8x10^6$ g)

1 $(V/T)*M*S*dw*C = mc$

2 $[mc/(mc + mk)]*100$ = wt% of component added to magma.

These calculations are only approximations because they consider only the major component added and ignore the effect of the other melted components on the density of the komatiitic magma because these effects are negligible for the amount of assimilation considered. The calculations were carried out for the Goethite member of the Jolliffe ore zone which has 59.08 wt % elemental Fe, has an estimated density of 4.2 gm/cc, and is

100 m thick (Shklanka, 1974). Dike widths from 0.3 to 10 m and their respective flow rates, from the model of Huppert and Sparks (1985b), are used to follow an eruption as it progressed. The Fe formation consists of goethite, hematite and minor quartz. Under high temperature conditions the goethite would probably dehydrate to from hematite. Hematite and tridymite melt to form a liquid in excess of 1400 °C at 1 bar pressure (Levin et al., 1964). However, a melting temperature of 1000 to 1400 °C for the Fe formation is used, to obtain an estimate on a range of reasonable melting rates from Figure 47, by taking into account possible effects of H_2O and other components in lowering the melting temperature. Calculations are presented for all reasonable melting rates for each flow rate. The lower melting rates would be most appropriate for the narrower dikes and the larger melting rates for thicker dikes.

The amount of FeO assimilated using formulae 1 and 2 is presented in Table 8. An inspection of these data shows that only at the very early stages of an eruption (0.3 m dike width) with high melting rates could any significant amount of Fe (1.88 wt%) have been added. The dike would rapidly grow to one meter thick for which even extremely high melting rates would add only insignificant amounts (0.64 wt%) of FeO. As the dike width grows further smaller percentages of FeO would be assimilated. It is therefore very unlikely that Fe-formation

dike width (d)	0.3	1	3	10
two dimensional flow rate (Q)	0.56	3.4	17.8	108
vertical velocity (V)	1.9	3.4	5.9	10.8
	wt% FeO	wt% FeO	wt% FeO	wt% FeO
MR(m/day)				
0.5	0.24			
1	0.47	0.08	0.015	
2	0.94	0.16	0.030	0.005
4	1.88	0.32	0.060	0.010
8		0.64	0.120	0.020

Table 8. **The range of wt% of FeO a komatiite magma might assimilate as it passes through 100m of iron formation present in the Steep rock Group at varying melting rates. MR=melting rate in meters/day; d=dike width in meters; Q=two deminsional flow rate (m^2/s); V=vertical velocity (m/s). Flow rate and vertical velocity from Huppert and Sparks, (1985a).**

contributed significantly to the observed Fe concentration in the Dismal Ashrock. There is no significant thickness of Fe formation found near the GUP, although the tectonized contacts of the GUP do not preclude an original assocaition.

The Mosher carbonate unit contains an average of 42.08 wt% CO_2 and is predominantly calcite with some minor areas of dolomite (Jolliffe, 1966). Calcite dissociates at 890°C and melts at 1340°C whereas dolomite disassociates at 780°C (Weast, 1988). If H_2O is present at 1000 bars pressure, calcite will begin to melt at 740°C (Wyllie and Tuttle, 1960). The carbonate package can be up to 500 m thick and has an assumed density of 2.7 gm/cc. Using formula 1 and 2 for various dike widths, unit thicknesses, and a wide range of melting rates the resultant wt% of CO_2 in the magma added by assimilation is calculated and presented in Table 9.

An inspection of the data shows that significant quantities of CO_2 could be added at the beginning stages of an eruption (up to 0.81 wt% for a conservative melting rate of two meters a day where a .3 m dike traversed only 250 m of carbonate). For a three meter wide dike traversing 500 m of carbonate at a melting rate of four meters a day, 0.106 wt% CO_2 could have been assimilated. Approximately an equal amount of CaO would also be assimilated. There are no experimental data of CO_2 solubility specfically in komatiites at low pressures, however, the solubility of CO_2 in basic and ultrabasic magmas

dike width (d)		0.3	1	3	10
two dimensional flow rate (Q)		0.56	3.4	17.8	108
vertical velocity (V)		1.9	3.4	5.9	10.8
MR(m/day)	T(m)	wt% CO2	wt% CO2	wt% CO2	wt% CO2
0.5	250	0.21			
	500	0.41			
1	250	0.41	0.07	0.013	
	500	0.81	0.14	0.026	
2	250	0.81	0.14	0.026	0.004
	500	1.62	0.29	0.053	0.008
4	250	1.62	0.29	0.053	0.008
	500	3.24	0.58	0.106	0.016
8	250		0.58	0.106	0.016
	500		1.16	0.210	0.032

Table 9. **The range of wt% of CO_2 a komatiite magma might assimilate as it passes through either 250 m or 500 m of carbonate in the Steep Rock Group at varying melting rates. Abbreviations as in Table 8.**

has been calculated to be very low (<0.20 wt%) at low (<500 bars) pressure (Spera and Bergman, 1980). Measured solubility of CO_2 in basalts at quench temperatures ranged from 0.0062 wt% at 100 bars to 0.028 wt % at 500 bars (Harris, 1981). Provided that small amounts of carbonate rock are miscible in komatiite magma, the assimilated CO_2 probably assisted the vesiculation of the magma and production of phreatomagmatic activity at an early stage of the eruption. However, juvenile volatiles cannot be ruled out and are a likely possibility. No significant quantities of carbonate rocks are now spatially associated with the GUP, although the tectonized contacts of the GUP does not preclude an original association.

III. 4 Source of the Magma

An enriched mantle source could explain most of the features of the GUP and Dismal Ashrock. Since komatiites are produced by high degrees of partial melting of mantle peridotite the abundance of incompatible elements such as Ti and Zr probably reflect source regions (Sun, 1987). Therefore the Dismal Ashrock and GUP, which are rich in these and other incompatible elements, were likely the result of magma produced from an enriched mantle and this indicates that the Archean mantle was heterogeneous. However, heterogeneity in an Archean mantle is counter to some recent thinking of a very hot, very fluid and homogeneous mantle during the Archean. For example,

Nisbet and Walker (1982) have proposed the existence a global magma ocean that formed during the formation of the earth and lasted until the end of the Archean.

An enriched mantle can be produced by a number of mechanisms. For example Sun (1987) has suggested lithosphere subduction, melt migration and mantle metasomatism as possible mechanisms. Anderson (1982) has proposed a global primary enriched mantle to explain ancient enriched mantle.

No determination can be made on the cause of enriched mantle in the case of the Steep Rock and GUP without isotopic data. However, considering the unusual array of elements in which the magma was enriched (Fe, Ti, Zr, Ba, Sr, Nb, Rb and possibly volatiles) a mantle metasomatic event seems a distinct possibility. How a portion of the Archean mantle could be enriched and maintain its heterogeneity in the presence of strong mantle convection is not understood. However, there is evidence for Precambrian and perhaps Archean mantle enrichment events. For example McCulloch, Jaques, Nelson, Lewis (1985) have proposed that a mantle enrichment of Archean age is responsible for the production of kimberlites and lamproites in the west Kimberley area of Western Australia based on Nd and Sr data.

Though much of the above discussion concerning the Dismal Ashrock and GUP has to be considered speculative, there is good evidence that the source region for the Dismal Ashrock and GUP

was enriched in incompatible elements.

The mafic flows, blocks and dikes within the Dismal Ashrock show no enrichment of these elements and therefore could not have been produced from an enriched mantle. Therefore, the enriched portion of the mantle would have to have been limited in size, so that the parental magmas to the basalts did not tap this source region.

IV CONCLUSIONS

There are three major conclusions to this study:

1) The Dismal Ashrock and the GUP have the same remarkable array of physical and chemical features that are rare or unique on a global scale (Table 10) which indicate that they are correlative in some manner. However, there are some differences between the two units. For example the Dismal Ashrock contains a mafic flow, komatiitic volcaniclastic rocks and alteration zones not found in the GUP. In addition the Dismal Ashrock is part of a supracrustal sequence, thought to be formed in a rift basin (Wilkes, 1986), that overlies a granitic basement. The GUP is not part of such a sequence but its highly strained contacts allow no conclusive determination of its primary relationship, if any, to surrounding units. There are three possible models that could explain these differences between the units and their present separation.

First, the two units were once connected but the dextral Quetico fault could have had a vertical component of movement which would result in the exposure of different parts of an original komatiitic pyroclastic rock unit. Therefore, the laterally discontinuous units in the Dismal Ashrock and the underlying supracrustal sequence of the Steep Rock Group are not present in or below the GUP. This view emphasizes a simplistic view of late dextral motion on the Quetico fault.

TABLE 10
CHARACTERISTICS OF THE DISMAL ASHROCK AND GUP

	Dismal Ashrock	GUP
Komatiitic (MgO>18 wt %; high Ni and Cr)	yes	yes
Juvenile pyroclasts	yes	yes
Cored and composite lapilli	yes	yes
Contain vesicular pyroclasts	yes	yes
High Fe, MnO	yes	yes
High Zr, Ti, Nb and P2O5	yes	yes
High Rb, and Ba	yes	yes
High K	yes	no
Accidental carbonate fragments	yes	yes
Accidental Tonalite fragaments	yes	no
Mafic flow	yes	no
Komatiitic volcaniclastic rocks	yes	no
Contains pyrite and Fe depleted alteration	yes	no
Part of a supracrastal sequence overlying a major unconformity	yes	?

Second, The GUP and the Dismal Ashrock could represent different originally separate areas where komatiitic magma from enriched mantle sources was erupted and both of these areas contained carbonate rocks (to account for the accidental carbonate fragments). In this model the Dismal Ashrock and GUP were not part of an original komatiitic unit that was broken up by tectonic processes, but rather they were derived from the same type of mantle. This model is least likely in that it requires the coincidence of two similarly enriched source regions or single but very large enriched source region. Third, an original komatiitic pyroclastic rock unit was split into an upper GUP and lower Dismal Ashrock by thrust faults before late movement on the Quetico fault. The shear zones at the top of the Dismal Ashrock and on both sides of the GUP may be evidence for an early thrusting event. This model would be consistent with a transpressive tectonic regime.

2) The Dismal Ashrock and the GUP were both produced by phreatomagmatic explosive volcanism. The water-magma interaction was probably induced by the exsolution of the volatiles and the resultant modification of eruption parameters.

3) The Dismal Ashrock and GUP are enriched in incompatible elements. This enrichment could not have been produced by alteration nor assimilation, therefore an enriched mantle source region for these magma is inferred.

REFERENCES

Anderson, D. C., 1980. Isotopic evolution of the mantle: role of magma mixing, Earth Planetary Science Letters, v. 57, pp. 1 - 12.

Arndt, N. T., Francis D., and Hynes, A. J., 1979. The field characteristics and petrology of Archean and Proterozoic komatiites, Canadian Mineralogist, v. 17, pp. 147 - 163.

Arndt, N. T., Naldrett, A. J., and Pyke, D. R., 1977. Komatiitic and iron rich tholeiitic lavas of Munro Township, northeast Ontario, Journal of Petrology, v. 18, pp. 319 - 369.

Arndt, N. T., and Nesbitt, R. W., 1982. Geochemistry of Munro Township basalts, in Arndt, N. T., and Nisbet, E. G., Komatiites, George Allen and Unwin, London, pp. 309 - 329.

Arth, J. G., Arndt, N. A., and Naldrett, A. J., 1977. Genesis of Archean komatiites from Munro Township Ontario: trace element evidence, Geology, v. 5, pp. 590 - 594.

Barnes, R. G., Lewis, J. D., and Gee, R. D., 1974. Archean ultramafic lavas from Mount Clifford, Western Australia Geological Survey Annual Report, n. 1973, pp. 59 - 70.

Bartley, M. W., 1940, Iron deposits of the Steep Rock Lake area, Ontario Department of Mines, v. 48, pp. 35 - 47.

Blackburn, C. E., Bond, W. D., Breaks, F. W., Davis, D. W., Edwards G. R., Poulsen, K. H., Trowell, N. F., and Wood, J., 1985. Evolution of archean volcanic - sedimentary sequences of the western Wabigoon Subprovince and its Margins: a review, Geological Association of Canada Special Paper 28, pp. 89 - 116.

Brooks, C., James, D. E., and Hart, S. R., 1976. Ancient lithosphere: its role in young continental volcanism, Science, v. 193, pp. 1086 - 1094.

Card, K. D., and Ciesielski, A., 1986. Subdivisions of the Superior Province of the Canadian Shield, Geoscience Canada, v. 13, pp. 5 - 13.

Collerson, K. D., and Bridgewater, 1979. Metamorphic development of early Archean tonalitic and trondhjemitic gneisses, Saglek area Labrador, in Barker, F., ed., Trondhjemites, Dacites and Related Rocks, Elsevier Scientific Publishing Company, New York, pp. 205 - 265.

Echevervia, L. M., and Aitken, 1986. Pyroclastic rocks: another manifestation of ultramafic volcanism on Gorgona Island Columbia, Contributions to Mineralogy and Petrology, v. 92, pp. 428 - 436.

Eckstrand, R. O., and Williamson, B. L., 1985. Vesicles in the Dundonald Komatiites (abstract) in GAC, MAC, CGU Joint Annual Meeting 10, p. A16.

Ermanovics, I. F., McRitchie, W. D., and Houston, L., 1979. Petrochemistry and tectonic settings of plutonic rocks of the Superior Province in Manitoba, in Barker f., ed, Trondhjemites, Dacites and Related Rocks, Elsevier Scientific Publishing Company, New York, pp. 323 - 358.

Gelinas, L., Lajoie, J., and Brooks, C., 1976. The origin and significance of Archean ultramafic volcaniclastics from Spinifex Ridge, Lamotte Township, Quebec, Geological Association of Canada Special Paper, n. 16, pp. 227 - 309.

Grant, J. A., 1986. The Isocon diagram - A simple solution to Gresens Equation for metasomatic alteration, Economic Geology, v. 81, pp. 1976 - 1982.

Green, J. C., and Schulz, K. J., 1977. Iron-rich basaltic komatiites in the early Precambrian Vermilion District, Minnesota, Canadian Journal of Earth Sciences, v. 14, pp. 2181 - 2192.

Gresens, R. L., 1967. Composition - volume relationship of metasomatism: Chemical Geology, v. 2, pp. 47 - 55.

Harris D. M., 1981. The concentration of CO_2 in submarine tholeiitic basalts, Journal of Geology, v. 89, pp. 689 - 701.

Harris, F. R., 1974. Geology of the Rainy Lake area District of Rainy River, Ontario Division of Mines Geological Report 115, 94 p.

Huppert, H. E., and Sparks, R. S. J., 1985a. Komatiites I eruption and flow, Journal of Petrology, v. 26, pp. 694 - 725.

Huppert, H. E., and Sparks, R. S. J., 1985b. Cooling and contamination of mafic and ultramafic lavas during ascent through the continental crust, Earth and Planetary Science Letters, v. 74, pp. 371 - 386.

Jahn, B.-M., Gruau G., and Glikson, A. Y., 1982. Komatiites of the Onverwacht Group, South Africa: REE geochemistry, Sm/Nd age and mantle evolution, Contributions to Mineralogy and Petrology, v. 80, pp. 25 - 40.

Jensen, L. S., 1976. A new cation plot for classifying subalkalic volcanic rocks, Ontario Division of Mines and Miscellaneous Paper 66.

Jolliffe, A. W., 1966. Stratigraphy of the Steep Rock Group, Steep Rock Lake, Ontario, in Precambrian Symposium, Goodwin, A. W., Geological Association of Canada Special Paper, n. 3, pp. 75 - 98.

Jolliffe, A. W., 1955. Geology and iron ores of Steep Rock Lake, Economic Geology, v. 50, pp. 376 - 389.

Jolliffe, T. S., 1971. The character of the Steeprock Ashrock, Bachelor of Science Thesis, Queens University, Kingston Ontario, 47 p.

Kokelaar, P., 1986, Magma water interactions in subaqueous and emergent basaltic volcanism, Bulletin of Volcanology, v. 48, pp. 275 - 289.

Lawson, A. C., 1912. Geology of the Steep Rock Lake, Ontario, Geological Survey of Canada Memoir 28, pp. 7 - 15.

Lewis, J. D., and Williams I. R., 1973. The petrology of an ultramafic lava near Murphy Well eastern Goldfields, Western Australia, Western Australia Geological Survey Annual Report, n. 1972, pp. 60 - 68.

Levin, E. L., Robbins, C. R., and McMurdie, H. F., 1964. Phase diagrams for Ceramicists, The American Ceramic Society, Columbus, Ohio, 574p.

Lorenz, V., 1975. Formation of phreatomagmatic maar-diatreme volcanoes and its relevance to kimberlite diatremes, Physics and Chemistry of the Earth, v. 9, pp. 17 - 27.

McCulloch, M. T., Jaques, A. L., Nelson, D. R., and Lewis, J. D., 1983. Nd and Sr isotopes in kimberlites and lamproites from Western Australia: an enriched mantle origin, Nature, v. 302, pp. 400 - 403.

McIntosh, J. R., 1974. The Cayland Ore Company Limited deposit: a geologic description, in Shklanka, R., Geology of the Steep Rock Lake area District of Rainy River, Ontario Department of Mines and Northern Affairs Geologic Report 93, pp. 83 - 105.

Nesbitt, R. W., and Sun, S. S., 1976. Geochemistry of Archean spinifex textured peridotite and magnesian and low magnesian tholeiites, Earth and Planetary Science Letters, v. 31, pp. 433 - 453.

Nisbet, E. G., and Walker, D., 1982. Komatiites and the structure of the Archean mantle, Earth and Planetary Science Letters, v. 60, pp. 105 - 113.

Poulsen, K. H., 1986. Rainy Lake wrench zone: An example of an Archean subprovince boundary in Northwestern Ontario (abstract), Workshop on the Tectonic Evolution of Greenstone Belts, Lunar Planetary Institute, Houston, Jan. 16.

Poulsen, K. H., 1984. Archean tectonics and mineralization at Rainy Lake, northwestern Ontario, unpublished Ph.D. Thesis, Queen's University, Kingston Ontario, 342p.

Poulsen, K. H., Borradaile G. J., and Kehlenbeck, M. M., 1980. An inverted Archean succession at Rainy Lake, Ontario, Canadian Journal of Earth Science, v. 17, pp. 1358 - 1369.

Ramsay, J. G., and Huber, M. I., 1987. The Techniques of Modern Structural Geology v. 2, Academic Press, New York, 697p.

Saverikko, M., 1985. The pyroclastic komatiite complex at Sattasvaara in northern Finland, Bulletin of the Geological Society of Finland, v. 57, pp. 55 - 87.

Saverikko, M., 1983. Explosive komatiitic volcanism in the Finnish Lapland, Geologi, v. 5, pp. 21 - 23.

Schulz, K. J., 1982, Magnesian basalts from the Archean terrains of Minnesota, in Arndt, N. T., and Nisbet, E. G., Komatiites, George Allen and Unwin, London, pp. 171 - 186.

Sheridan, M. F., and Wohletz, K. H., 1983. Hydrovolcanism: basic considerations and review, Journal of volcanology and Geothermal Research, v. 17, pp. 1 - 30.

Shklanka, R., 1972. Geology of the Steep Rock Lake area, District of Rainy River, Ontario Department of Mines and Northern Affairs Geological Report, n. 93, pp. 1 - 84.

Smith, W. H. G., 1893. The Archean rocks west of Lake Superior, Geological Society of America Bulletin, v. 4, pp. 338 - 438.

Smyth, H. L., 1891. Structural geology of Steep Rock Lake, Ontario, American Journal of Science - Third Series, v. XLII, n. 250, pp. 317 - 331.

Spera, F. J., and Bergman, S. C., 1980. Carbon dioxide in igneous petrogenesis I, Contributions to Mineralogy and Petrology, v. 74, pp. 55 - 66.

Stone, W. E., Jensen, L. S., and Church, W. R., 1987. Petrography and geochemistry of an unusual Fe- rich basaltic komatiite from Boston Township, northeastern Ontario, Canadian Journal of Earth Sciences, v. 24, pp. 2537 - 2550.

Sun, S.-S., 1987. Chemical composition of Archean komatiites: implications for early history of the earth and mantle evolution, Journal of Volcanology and Geothermal Research, v. 32, pp. 67 - 82.

Tarney, J., Weaver, B., Drury, S. A., 1979. Geochemistry of Archean trondhjemitic and tonalitic gneisses from Scotland and east Greenland, in Barker F., ed. Trondhjemites, Dacites and Related Rocks, Elsevier Scientific Publishing Company, New York, pp. 323 - 358.

Viljoen, M. J., and Viljoen, R. P., 1969. The geology and geochemistry of the lower ultramafic unit of the Onverwatcht Group and a proposed new class of igneous rock, Geological Society of South Africa Special Publication, n. 2, pp. 55 - 85.

Warren, P. H., 1984. Primordial degassing, lithosphere thickness and the origin of komatiites, Geology, v. 12, pp. 335 - 338.

Weast, R. C., 1988. Handbook of Chemistry and Physics, The Chemical Rubber Co., Cleveland.

Wilkes, M. E., 1986. The geology of the Steep Rock Group, N. W. Ontario: A major Archean unconformity and Archean stromatolites, Unpublished Master of Science Thesis, University of Saskatchewan, Saskatoon, 212p.

Wilkes, M. E., and Nisbet, E. G., 1987. Stratigraphy of the Steep Rock Group, northwest Ontario, A major Archean unconformity and Archean stromatolites, Canadian Journal of Earth Sciences, v. 25, pp. 370 - 391.

Wilson, L., Head, J. W., 1981. Ascent and eruption of basaltic magma on the earth and moon, Journal of Geophysical Research, v. 86, pp. 2971 - 3001.

Wilson, M., 1989. Igneous Petrogenesis, Unwin Hyman, Boston, 466p.

Wohletz, K. H., 1986. Explosive magma-water interactions: Thermodynamics, explosion mechanisms and field studies, Bulletin Volcanology, v. 48, pp. 245 - 264,

Wohletz, K. H., 1983. Mechanisms of hydrovolcanic pyroclast formation: grain-size, scanning electron microscopy and experimental studies, Journal of volcanology and Geothermal Research, V. 17. pp. 31 - 64.

Wright , C. M., 1965. Syngenetic pyrite associated with a Precambrian iron ore deposit, v. 57, pp. 1 - 12.

Wright, C. M., 1959. Pyrite zones in the hanging wall of the Steep Rock ore zone, Unpublished Masters of Science Thesis, Queens University Kingston, Ontario.

APPENDIX I

SUMMARY OF PETROGRAPHIC ANALYSIS OF THE DISMAL ASHROCK AND THE GUP

A summary of the petrography of the Dismal Ashrock and the GUP is presented in Tables 1 and 2 respectively. The following abbreviations are used:

Units

LT	= Komatiitic lapilli tuff
VB	= Komatiitic volcanic breccia
KV	= Komatiitic volcaniclastic rocks
Mf	= Mafic lava flow

Alt = Alteration types

FD	= Fe - depleted
OX	= Oxidized

Minerals

T-A	= Tremolite - actinolite
CHL	= Chlorite
SERP	= Serpentine
TALC	= Talc
OPAQ	= Opaques
CARB	= Carbonate
PLAG	= Plagioclase
DIOP	= Diopside
SPHN	= Sphene
HNBLD	= Hornblende
QTZ	= Quartz
BTE	= Boitite
GRDMASS	= Groundmass

APPENDIX I
TABLE 1

PETROGRAPHY OF THE DISMAL ASHROCK

SAMPLE	UNIT	ALT	T-A	CHL	SERP	TALC	OPAQ	CARB	PLAG	DIOP	SPHN	HNBLD	QTZ	BTE	GRDMA
KOMATIITIC PYROCLASTIC ROCKS															
SRE-2	LT		40	11	20	10	15	3			1				
SRE-11	LT		35	6	14		22	23							
SRE-14	LT	FD	30	5	13		10	35					7		
SRE-21	LT		5	20	20	5	10	40							
SRE-45	LT	FD	31	15	20		9	23					2		
SRE-70	LT		44	14	25		15	10							
SRE-73	LT	OX	36	30	8		16	10							
SRE-224	LT		10	20		20	20	30							
SRE-229	LT		5	34	5	10	15	30					1		
SC-300	LT		5	10	18	20	17	30							
SRE-65A	VB		34	6	25		25	10							
SRE-65D	VB		38	20	10		22	10							
KOMATIITIC VOLCANICLASTIC ROCKS															
SRE-71	KV		58	2	20		20								
SRE-230	KV			10	30		15	45							
SRE-231	KV				64		16						20		
SRE-232	KV				25		15	60							
MAFIC FLOW AND BLOCK															
SRE-18	MF			20			5	5	40						30
SRE-68	VB			25			5	5	40			25			
SRE-91	MF			29			1	10	15			15			30
MAFIC DIKES															
SRE-8			30	48			4	10			1		7		
SRE-84			4	37			10	26					23		

APPENDIX I
TABLE 2

PETROGRAPHY OF THE GRASSY PORTAGE BAY ULTRAMAFIC PYROCLASTIC ROCK UNIT

SAMPLE	UNIT	ALT	T-A	CHL	SERP	TALC	OPAQ	CARB	PLAG	DIOP	SPHN	HNBLD	QTZ	BTE	GRDMS
GREEN KOMATIITIC PYROCLASTICS															
SS-542B	LT			34	21			12	3		25	5			
SS-544	LT			43	20			10	5		17	5			
SS-549	LT			42	26		20	10			2				
SS-563	LT				20			10	2		13	5	50		
GREY KOMATIITIC PYROCLASTICS															
SS-506	LT				95			5							
SS-509	LT			53	27		2	18							
SS-512	LT			40	30		20	10							
SS-516A	LT			50	30		5	15							
SS-516B	LT			52	25		5	18							
SS-517	LT			35	17		30	18							
SS-523	LT	OX		40	30		10	20							
SS-554	LT			58	13			22	5			2			
SS-565	LT	OX		58	15		5	22							
SS-518	VB			54	15		10	21							
SS-530	VB			38	20		17	25							
MAFIC DIKE															
SS-529	MD									20		5	69		6
SS-542a	MD								4	48		4	44		

The following elements are in parts per million (ppm)

	Method	DL ppm
Ni	DCP	1
Cr1	DCP	2
Cr2	XRF	2
Co	DCP	1
Cu	DCP	0.5
V	DCP	2
Y1	XRF	2
Y2	XRF	2
Zr1	XRF	3
Zr2	XRF	3
Nb1	XRF	2
Nb2	XRF	2
Ba	XRF	10

LOI *(see next page)

The following abreviations are used:

Units
- LT = Komatiitic Laplli tuff
- VB = Komatiitic Volcanic Breccia
- KV = Komatiitic Volcaniclastic Rocks
- MF = Mafic Lava Flow
- MD = Mafic dikes
- KM = Mafic volcanics and intrusives

Alt = Alteration Type
- FD = Fe depleted
- OX = Oxidized

SType = Sample Type (no symbol indicates a whole rock sample)

- CLF = Cognate laplli fragment
- JLF = Juvenile lapilli fragment
- LF = Lapilli fragment, undifferentiated
- B = Volanic block, undifferentiated
- JB = Juvenile bomb

\- = less than (<)

* NOTE ON LOSS ON IGNITION VALUES

The loss on ignition (LOI) reported in tables 1 and 2 of this appendix is the weight loss induced by a roasting process; it does not take into account the oxidation of FeO (weight gain) that will occur during the roasting process. A corrected loss on ignition (CLOI) is obtained by determining the weight gain from oxidation of FeO (original FeO value obtained by wet chemical analysis) in the sample, which is then added to the original loss on ignition value. This corrected loss on ignition value (CLOI) and the resultant total is used in this thesis for all volatile free calculations.

APPENDIX II
TABLE 1
RESULTS OF MAJOR ELEMENT ANALYSIS (XRF) OF THE DISMAL ASHROCK

Samp #	Unit	Alt	SType	SiO2	MgO	Al2O3	CaO	Fe2O3t	MnO	Na2O	K2O	TiO2	P2O5	LOI	TOTAL	CLOI
KOMATIITIC PYROCLASTIC ROCKS																
sre-2	LT			38.00	14.70	3.94	13.80	14.90	0.30	0.38	0.20	1.30	0.10	10.80	98.42	11.94
sre-14	LT	FD		42.00	8.26	3.97	13.60	9.10	0.32	0.01	0.41	1.32	0.09	20.90	99.98	21.62
sre-45	LT	FD		33.90	20.00	4.39	9.03	13.30	0.14	0.12	0.18	1.48	0.12	15.30	97.96	16.00
sre-65	VB			40.40	16.20	4.17	10.50	16.40	0.28	0.24	0.67	1.36	0.09	7.77	98.08	8.94
sre-67	LT			26.40	16.50	12.00	10.60	16.40	0.20	0.13	1.31	0.87	0.36	14.20	98.97	15.47
sre-70	LT			42.80	18.60	4.49	7.26	17.20	0.26	0.23	0.48	1.51	0.12	5.16	98.11	6.23
sre-73	LT	OX		36.90	17.00	4.51	9.31	18.00	0.26	0.13	0.18	1.49	0.11	10.30	98.19	11.16
sre-81	LT			39.20	20.80	4.81	4.04	16.70	0.23	0.09	0.03	1.60	0.11	10.60	98.21	11.88
sre-215	LT			33.10	12.60	4.20	12.30	14.70	0.43	-0.01	0.11	1.44	0.12	20.20	99.19	21.39
sre-220	LT			32.60	10.20	4.33	16.90	14.90	0.28	0.11	0.65	1.63	0.16	16.60	98.36	17.69
sre-224	LT			34.10	9.59	3.58	16.20	15.40	0.31	0.13	0.95	1.17	0.10	16.70	98.23	17.84
88-ss-225	LT			35.20	8.42	3.29	17.50	14.80	0.24	0.17	0.76	1.12	0.09	17.40	98.99	18.47
sre-229	LT			32.40	10.80	3.37	14.00	14.60	0.39	0.02	0.37	1.14	0.08	22.40	99.57	23.58
sc-300	LT			35.20	8.13	3.41	19.50	14.20	0.32	0.09	0.13	1.07	0.09	17.20	99.34	18.01
sre-665-c	VB		CLF	35.00	17.40	7.48	4.06	22.90	0.19	0.17	0.71	2.32	0.73	6.08	97.04	7.71
sre-665-j	VB		JLF	37.40	16.50	5.78	7.73	19.50	0.25	0.57	0.88	1.73	0.40	7.39	98.13	8.83
KOMATIITIC VOLCANICLASTIC ROCKS																
sre-71	LT			35.60	14.10	3.51	5.58	34.10	0.30	0.16	0.10	0.81	0.07	3.62	97.95	5.21
sre-92	KV			35.90	13.30	3.63	11.20	14.60	0.35	-0.01	0.11	1.09	0.10	19.10	99.37	20.00
88-ss-230	KV			24.80	13.30	4.33	15.90	12.50	0.48	-0.01	0.04	1.19	0.09	25.90	98.52	26.77
sre-231c	KV			46.10	4.95	6.99	0.33	33.50	0.13	0.03	0.02	0.33	0.10	6.00	98.48	7.02
88-ss-232a	KV			41.50	10.70	6.26	8.53	14.30	0.37	0.04	0.02	1.93	0.14	15.20	98.99	16.27
sc-303	KV			43.30	18.20	5.02	6.86	16.80	0.19	0.36	0.03	1.26	0.11	3.85	95.98	4.84
MAFIC FLOW AND BLOCK																
sre-18	MF			35.90	11.00	13.80	4.03	20.30	0.51	-0.01	0.27	0.93	0.05	11.70	98.48	13.53
sre-68	VB			45.50	8.52	13.10	5.73	12.50	0.20	4.26	0.98	0.90	0.08	6.77	98.54	7.73
sre-91	MF			46.20	6.95	13.90	9.19	11.90	0.21	1.16	0.20	0.82	0.06	8.77	99.36	9.74
MAFIC DIKES																
sre-8				38.10	13.90	14.80	0.55	20.60	0.16	0.05	0.47	1.10	0.10	8.23	98.06	10.09
sre-62				48.20	5.60	11.80	8.42	6.84	0.14	5.61	1.40	0.76	0.59	6.77	96.13	7.05
sre-84				45.70	4.30	11.80	7.40	14.90	0.21	1.37	0.21	1.68	0.13	10.80	98.50	12.17
sre-217				30.80	11.20	11.10	9.30	14.60	0.26	0.02	0.12	0.74	0.75	19.10	97.99	20.00
CARBONATIZED SHEAR ZONE ROCKS																
sre-211				4.44	11.90	1.32	26.20	13.30	0.84	0.05	0.25	0.85	0.03	39.20	98.38	40.41
sre-214				1.30	12.10	0.15	26.70	16.00	1.48	0.04	0.04	0.06	0.05	36.00	93.92	37.17

APPENDIX II
TABLE 2

RESULTS OF MAJOR ELEMENT CHEMICAL ANALYSIS (XRF) OF THE GUP

Samp #	Unit	Alt	S Type	SiO2	MgO	Al2O3	CaO	Fe2O3t	MnO	Na2O	K2O	TiO2	P2O5	LOI	TOTAL	CLOI
GREEN KOMATIITIC PYROCLASTIC ROCKS																
88-ss-528	LT			46.60	10.70	6.36	12.00	19.30	0.24	0.76	0.35	1.27	0.05	0.70	98.32	2.30
88-ss-542b	LT			39.70	13.80	4.74	12.60	20.10	0.18	0.32	0.11	1.17	0.11	2.16	94.99	3.27
88-ss-544	LT			40.30	12.70	5.03	14.00	20.70	0.18	0.43	0.11	1.20	0.15	1.85	96.65	3.10
88-ss-563	LT			38.60	7.27	5.93	13.40	28.30	0.21	0.73	0.38	1.18	0.08	0.00	96.07	1.84
88-ss-744	LT		LF	41.30	14.40	8.26	10.20	16.50	0.19	0.58	0.24	0.75	0.02	3.08	95.51	4.36
GREY KOMATIITIC PYROCLASTIC ROCKS																
88-ss-506	LT			27.50	22.60	17.10	0.11	17.80	0.10	0.08	0.02	0.67	0.09	10.30	96.37	11.91
88-ss-512	LT			41.00	19.70	5.78	5.91	16.40	0.28	0.19	0.03	1.38	0.11	4.62	95.40	5.63
88-ss-516	LT			40.70	22.30	5.31	3.28	16.60	0.26	0.13	0.02	1.45	0.09	5.47	95.61	6.46
88-ss-518	VB			41.70	21.20	5.45	5.04	17.60	0.30	0.12	0.07	1.66	0.12	5.23	98.49	6.25
88-ss-523	LT	OX		42.60	22.00	5.11	5.20	17.20	0.28	0.12	0.04	1.44	0.11	5.16	99.25	5.92
88-ss-549	LT			40.60	21.90	5.38	2.28	17.00	0.22	0.15	0.02	1.46	0.10	5.70	94.80	6.65
88-ss-561	LT			42.20	18.60	4.33	8.08	17.50	0.29	0.27	0.03	1.70	0.14	3.00	96.14	3.94
88-ss-562b	LT			43.60	20.90	4.98	6.87	12.30	0.26	0.20	0.04	1.41	0.11	5.08	95.74	6.08
88-ss-565	LT	OX		40.00	23.60	3.56	5.39	18.70	0.29	0.14	0.02	1.55	0.12	5.62	98.99	6.34
88-ss-580	VB		B	41.90	20.00	4.91	6.90	15.80	0.42	0.28	0.03	1.76	0.13	4.16	96.29	5.12
88-ss-581	VB		JB	43.40	18.80	3.55	7.98	17.20	0.36	0.33	0.03	1.55	0.09	3.08	96.37	3.98
ss-ssj-716	VB		JLF	44.00	21.50	4.45	6.55	12.90	0.38	0.27	0.03	1.97	0.13	4.16	96.33	4.98
MAFIC ROCKS																
88-ss-529	MD			42.70	6.60	13.10	13.20	18.00	0.25	0.94	0.67	1.42	0.10	1.16	98.14	2.62
88-ss-542a	LT			47.30	6.97	13.50	12.50	12.40	0.20	1.77	0.96	0.83	0.07	1.70	98.19	2.78
88-ss-562a	KM			49.00	7.35	14.10	10.80	12.00	0.21	2.51	0.49	0.87	0.07	1.00	98.40	2.00

APPENDIX II
TABLE 3

WET CHEMICAL ANALYSIS OF THE DISMAL ASHROCK

Sample #	FeO	Fe2O3	H2O+	CO2
KOMATIITIC PYROCLASTIC ROCKS				
sre-2	10.20	3.56	3.10	7.17
sre-14	6.50	1.88	1.30	19.70
sre-45	6.30	6.30	3.80	10.50
sre-65	10.60	4.61	2.90	4.10
sre-67	11.40	3.73	6.00	7.55
sre-70	9.60	6.53	2.90	0.50
sre-73	7.70	9.44	4.20	4.62
sre-81	11.50	3.92	4.80	5.95
sre-215	10.70	2.81	3.20	18.00
sre-220	9.80	4.01	4.50	12.30
sre-224	10.20	4.06	4.20	12.10
88-ss-225	9.60	4.13	3.10	12.00
sre-229	10.60	2.82	2.60	20.20
sc-300	7.30	6.09	2.60	14.70
src-665-cog	14.60	6.68	6.30	0.14
srj-665-juv	12.90	5.16	4.90	2.68
KOMATIITIC VOLCANICLASTIC ROCKS				
sre-71	14.30	18.21	3.10	0.04
sre-92	8.10	5.60	2.90	16.50
88-ss-230	7.80	3.83	3.00	23.50
sre-231c	9.20	23.28	6.20	0.22
88-ss-232a	9.60	3.63	3.50	12.10
sc-303	8.90	6.91	3.80	0.05
MAFIC FLOW AND BLOCK				
sre-18	16.40	2.08	6.50	5.59
sre-68	8.60	2.94	2.80	3.59
sre-91	8.70	2.23	4.10	4.49
MAFIC DIKES				
sre-8	16.70	3.90	8.40	0.28
sre-62	2.50	4.06	1.10	5.70
sre-84	12.30	1.23	4.40	6.91
sre-217	8.10	5.60	6.10	12.20
CARBONATIZED SHEAR ZONE ROCKS				
sre-211	10.90	1.19	0.30	40.90
sre-214	10.50	4.33	0.40	41.00

APPENDIX II
TABLE 4

WET CHEMICAL ANALYSIS OF THE GUP

GREEN KOMATIITIC PYROCLASTIC ROCKS

Sample #	FeO	Fe2O3	H2O+	CO2
88-ss-528	14.40	3.30	1.60	0.02
88-ss-542b	10.00	8.99	1.80	0.15
88-ss-544	11.20	8.25	2.20	0.08
88-ss-563	16.50	9.96	1.00	0.04
88-ss-744	11.50	3.72	3.50	0.03

GREY KOMATIITIC PYROCLASTIC ROCKS

88-ss-506	14.50	1.69	10.10	0.03
88-ss-512	9.10	6.29	4.20	0.02
88-ss-516	8.90	6.71	4.70	0.03
88-ss-518	9.20	7.38	4.60	0.02
88-ss-523	6.80	9.64	4.10	0.03
88-ss-549	8.50	7.55	5.40	0.01
88-ss-561	8.40	8.17	3.20	0.01
88-ss-562b	9.00	2.30	4.20	0.75
88-ss-565	6.50	11.48	5.20	0.01
88-ss-580	8.60	6.24	3.40	0.01
88-ss-581	8.10	8.20	2.60	-0.01
ss-ssj-716	7.40	4.68	3.90	1.89

MAFIC ROCKS

88-ss-529	13.10	3.44	1.60	0.09
88-ss-542a	9.70	1.62	1.80	0.03
88-ss-562a	9.00	2.00	1.10	-0.01

APPENDIX II
TABLE 5

TRACE ELEMENT DATA FOR THE DISMAL ASHROCK
DATA IN PPM EXCEPT S [WT%]

Sample #	Ni	Cr1	Cr2	Co	Cu	V	Y1	Y2	Zr1	Zr2	Nb1	Nb2	Rb	Sr	Ba	S
KOMATIITIC PYROCLASTIC ROCKS																
sre-2	1200	1700	1550	110	210	180	7	-10	56	51	16	19	20	106	22	0.03
sre-14	950	1800	1600	130	360	190	10	-10	60	59	23	32	26	15	86	0.06
sre-45	1300	1800	1760	230	180	210	9	-10	72	59	28	29	24	11	62	0.02
sre-65	1300	1600	1640	110	230	180	9	-10	57	58	15	18	25	75	55	0.05
sre-67	150	86	134	84	-1	160	20	24	105	102	11	21	71	377	193	0.01
sre-70	1200	2000	1800	120	280	170	12	19	80	60	15	18	31	36	81	0.05
sre-73	1200	1900	1740	130	180	190	7	-10	66	63	35	44	20	109	57	0.01
sre-81	1200	2000	1880	100	270	200	8	11	71	47	15	12	-10	94	57	0.02
sre-215	910	2000	1710	110	230	180	8	26	63	68	24	29	16	139	48	0.06
sre-220	830	2200	1950	99	280	220	9	11	63	65	13	17	37	97	18	0.03
sre-224	1100	1600	1490	120	200	150	6	-10	49	50	23	30	16	119	-10	0.04
88-ss-225	1100	1500	1370	100	200	160	9	14	38	37	11	19	21	112	-10	0.04
sre-229	840	1500	1370	90	200	140	8	-10	54	44	22	26	20	49	47	0.04
sc-300	960	1400	1280	89	50	150	10	-10	36	26	19	19	20	164	-10	0.02
src-665-cog	1700	14	63	150	960	280	19	16	188	176	22	32	39	15	110	0.06
srj-665-juv	1100	2100	1970	99	240	230	10	-10	99	81	19	27	44	88	121	0.03
KOMATIITIC VOLCANICLASTIC ROCKS																
sre-71	460	650	730	46	11	120	3	-10	56	38	18	22	30	-10	81	0.02
sre-92	810	1500	1500	67	160	140	10	-10	40	25	22	29	11	-10	47	0.02
88-ss-230	1100	1500	1410	110	290	200	7	-10	55	44	24	30	15	26	30	0.35
sre-231c	1600	430	472	71	360	180	6	-10	80	66	14	29	28	-10	103	0.05
88-ss-232a	310	1800	1740	170	490	270	10	-10	101	88	35	41	16	-10	44	0.26
sc-303	1300	1500	1390	97	230	160	10	18	67	47	20	22	13	-10	67	0.02
MAFIC FLOW AND BLOCK																
sre-18	260	280	330	74	59	290	11	11	40	19	15	19	27	-10	101	0.01
sre-68	250	280	321	72	140	250	15	19	42	32	5	-10	37	251	291	0.02
sre-91	140	250	290	59	140	260	14	13	22	13	13	11	24	75	37	0.04
MAFIC DIKES																
sre-8	420	420	515	96	34	280	5	-10	80	67	19	18	25	-10	89	0.01
sre-62	200	280	257	40	51	120	21	15	120	123	9	19	32	1100	16400	0.47
sre-84	32	16	40	58	110	400	27	10	80	72	14	25	10	47	30	0.02
sre-217	2800	680	679	170	140	140	25	20	120	122	19	22	-10	506	105	0.02
CARBONATIZED SHEAR ZONE ROCKS																
sre-211	670	1000	964	73	4	86	6	-10	42	44	8	-10	32	221	20	0.09
sre-214	38	16	19	10	42	24	7	-10	16	-10	14	18	-10	95	-10	1.60

APPENDIX II
TABLE 6

TRACE ELEMENT DATA FOR THE GUP
DATA IN PPM EXCEPT S [WT%]

Sample #	Ni	Cr1	Cr2	Co	Cu	V	Y1	Y2	Zr1	Zr2	Nb1	Nb2	Rb	Sr	Ba	S
GREEN KOMATIITIC PYROCLASTIC ROCKS																
88-ss-528	890	1600	1490	92	21	250	10	-10	51	54	22	27	12	18	41	0.01
88-ss-542b	1000	1500	1450	79	22	150	7	13	46	35	23	39	-10	-10	-10	0.01
88-ss-544	1300	1700	1410	94	64	170	4	15	47	48	10	17	14	-10	37	0.02
88-ss-563	890	1500	1320	100	25	120	11	-10	53	55	20	23	32	-10	76	0.07
88-ss-744	1200	460	509	100	1	130	12	-10	44	27	14	17	19	11	87	0.01
GREY KOMATIITIC PYROCLASTIC ROCKS																
88-ss-506	230	-2	57	81	-1	210	41	48	455	453	20	29	14	-10	118	0.01
88-ss-512	1000	1700	1660	88	160	160	11	-10	64	52	43	61	10	-10	45	0.05
88-ss-516	1300	1800	1650	110	120	150	7	14	74	68	24	26	-10	19	113	0.03
88-ss-518	880	1700	1700	82	22	180	14	-10	81	73	25	28	23	24	78	0.02
88-ss-523	1200	1800	1610	98	89	170	10	15	74	72	23	36	15	21	81	0.02
88-ss-549	1200	1800	1680	72	27	170	9	-10	65	44	34	41	17	-10	76	0.01
88-ss-561	560	1800	1720	63	51	190	9	15	81	68	36	31	12	21	62	0.02
88-ss-562b	1200	1900	1790	78	51	240	14	25	77	68	11	13	15	-10	45	0.08
88-ss-565	1300	1800	1750	85	81	110	9	-10	70	60	24	22	16	61	94	0.03
88-ss-580	790	1500	1380	82	590	160	12	-10	80	76	14	17	18	62	81	0.05
88-ss-581	750	1800	1650	77	52	160	12	18	64	55	25	29	-10	45	82	0.02
ss-ssj-716	940	1200	1070	89	42	140	19	27	95	85	20	28	-10	54	71	0.02
MAFIC ROCKS																
88-ss-529	120	120	138	67	14	410	10	20	24	17	5	-10	22	277	170	0.01
88-ss-542a	110	180	175	57	28	350	17	-10	26	23	6	15	40	110	235	0.01
88-ss-562a	120	270	286	55	90	330	19	31	33	28	13	15	19	112	116	0.08

APPENDIX II
TABLE 7
COMPARISON BETWEEN DUPLICATE ANALYSES

Four sets of blind duplicates were sent along with the rest of the samples to determine the reproducibility of the results. Presented in Table 7 are the four sets, along with the percentage difference (%DIFF) between the two analyses in each set. The final column is an average of the percentage difference (X%DIFF) for the four sets. Some elements have more than one analysis. The analyses used in this paper are denoted with a asterisk (*); if both analyses are denoted their average is used.

The reproducibility of all of the major elements and LOI, with the exception of Na_2O, K_2O and S, is good (<4.5 average percentage difference). The wet chemical analyses also produce acceptable results with the exception of H_2O. Trace element results are also good (< 15 average percent difference) with the exception of Y1, Y2 (most samples below detection limit), Ba, Nb1, Nb2, and Rb.

APPENDIX II
TABLE 7

COMPARISON OF DUPLICATE ANALYSES

	225	825	%DIFF	230	880	%DIFF	232	882	%DIFF	563	913	%DIFF		%%DIFF
Fe2O3t	14.80	15.00	1.3	12.50	12.40	0.8	14.30	14.10	1.4	28.30	28.20	0.4	Fe2O3t	1.0
Na2O	0.17	0.15	12.5	-0.01	-0.01	0.0	0.04	-0.01	120.0	0.73	0.71	2.8	Na2O	33.8
MgO	8.42	8.50	0.9	13.30	13.30	0.0	10.70	10.60	0.9	7.27	7.28	0.1	MgO	0.5
Al2O3	3.29	3.33	1.2	4.33	4.28	1.2	6.26	6.16	1.6	5.93	5.91	0.3	Al2O3	1.1
SiO2	35.20	35.40	0.6	24.80	24.80	0.0	41.50	40.90	1.5	38.60	38.60	0.0	SiO2	0.5
P2O5	0.09	0.10	10.5	0.09	0.09	0.0	0.14	0.13	7.4	0.08	0.08	0.0	P2O5	4.5
S	0.04	0.04	0.0	0.35	0.09	118.2	0.26	0.09	97.1	0.07	0.06	15.4	S	57.7
K2O	0.76	0.76	0.0	0.04	0.06	40.0	0.02	0.02	0.0	0.38	0.38	0.0	K2O	10.0
CaO	17.50	17.70	1.1	15.90	15.90	0.0	8.53	8.61	0.9	13.40	13.30	0.7	CaO	0.7
TiO2	1.12	1.15	2.6	1.19	1.18	0.8	1.93	1.91	1.0	1.18	1.18	0.0	TiO2	1.1
MnO	0.24	0.25	4.1	0.48	0.47	2.1	0.37	0.37	0.0	0.21	0.21	0.0	MnO	1.5
LOI	17.40	17.50	0.6	25.90	25.80	0.4	15.20	15.20	0.0	0.00	0.00	0.0	LOI	0.2
H2O+	3.10	3.50	12.1	3.00	3.00	0.0	3.50	4.00	13.3	1.00	0.70	35.3	H2O+	15.2
CO2	12.00	14.20	16.8	23.50	23.90	1.7	12.10	13.20	8.7	0.04	0.04	0.0	CO2	6.8
Fe2O3	4.13	4.11	0.5	3.83	3.62	5.6	3.63	3.99	9.4	9.96	9.76	2.0	Fe2O3	4.4
FeO	9.60	9.80	2.1	7.80	7.90	1.3	9.60	9.10	5.3	16.50	16.60	0.6	FeO	2.3
V	160	160	0.0	200	200	0.0	270	280	3.6	120	130	8.0	V	2.9
Cr1	1500	1700	12.5	1500	1600	6.5	1800	1900	5.4	1500	1600	6.5	*Cr1	7.7
Cr2	1370	1390	1.4	1410	1410	0.0	1740	1740	0.0	1320	1320	0.0	*Cr2	0.4
Co	100	100	0.0	110	110	0.0	170	160	6.1	100	110	9.5	Co	3.9
Ni	1100	1100	0.0	1100	1100	0.0	310	310	0.0	890	940	5.5	Ni	1.4
Cu	200	200	0.0	290	390	29.4	490	500	2.0	25	27	7.7	Cu	9.8
Rb	21	31	38.5	15	15	0.0	16	19	17.1	32	28	13.3	Rb	17.2
Sr	112	104	7.4	26	27	3.8	-10	-10	0.0	-10	-10	0.0	Sr	2.8
Y1	9	6	40.0	7	6	15.4	10	9	10.5	11	5	75.0	*Y1	35.2
Y2	14	-10	33.0	-10	-10	0.0	-10	-10	0.0	-10	-10	0.0	Y2	0.3
Zr1	38	45	16.9	55	53	3.7	101	78	25.7	53	57	7.3	*Zr1	13.4
Zr2	37	36	2.7	44	42	4.7	88	69	24.2	55	47	15.7	*Zr2	11.8
Nb1	11	23	70.6	24	25	4.1	35	23	41.4	20	20	0.0	*Nb1	29.0
Nb2	19	25	27.3	30	26	14.3	41	30	31.0	23	27	16.0	*Nb2	22.1
Ba	-10	-10	0.0	30	-10	100.0	44	35	22.8	76	97	24.3	Ba	38.0

APPENDIX III

The isocon method for determining mobile elements during metasomatic alteration.

Grant (1986) developed the isocon method to determine the chemical changes associated with metasomatic alteration by using chemical data from altered and unaltered samples that are assumed to be originally similar in composition. The isocon method allows for a rapid determination of elements that have been lost or gained during metasomatic alteration. The following is a description of the isocon method taken from Grant (1986).

The isocon method is based on Gresens' (1967) equations for determining changes in concentrations of components and the resultant volume change that occurred during metasomatic alteration. Gresens states that some components are likely to be immobile during alteration and once these components have been identified the amount of volume change can be established.

Grant (1986) has manipulated Gresens' equation 14 to produce a linear relationship that is the basis for the isocon method (eq. 2) (symbols listed in Table 1).

$$C^A = (M^O/M^A)\ (C^O + \Delta C) \qquad (1)$$

This equation can be written for each component and ΔC will be zero for those components that are immobile. The ratio M^O/M^A is constant and can be obtained by solving a set of simultaneous

equations for components where $\Delta C=0$. The simultaneous equations have the following form;

$$C^A = (M^O/M^A)C^O \qquad (2)$$

Table 1, Appendix III

Symbols used in equations (from Grant, 1986)

C = Concentration of a component

M = Mass of sample

O = Superscript for unaltered (original) sample

A = Superscript for altered (final) sample

M^O/M^A can also be determined graphically by plotting C^A against C^O for an immobile component. The slope of the line through an immobile component and the origin is M^O/M^A; this line is the isocon.

An isocon can be determined in this way by assuming the immobility of a certain element such as Al_2O_3 or by constructing a best fit line through a number of components that form a linear arrangement.

One of the most beneficial characteristics of the isocon method is it produces a graphical image that can be quickly interpreted. For example those elements that have slopes

greater than that of the reference isocon have been gained during alteration whereas those components that have slopes less than the reference isocon have been lost. The greater the difference in the slope of a component to the reference isocon the greater the relative change in the concentration of that component. Since the slope is the determinant the concentration of components (with a wide range of values) can be scaled to fit on one graph. For this thesis major and trace element data are plotted on a graph that range from 0-50 wt% and 0-50ppm. The reference isocon can have slopes greater or less than one representing mass loss and gain respectively.